Commun. Optim. Theory 2025 (2025) 24 https://doi.org/10.23952/cot.2025.24

Communications in Optimization Theory
Available online at http://cot.mathres.org

NUMERICAL STUDY OF A THREE-DIMENSIONAL REACHABLE SET FOR A DUBINS CAR UNDER AN INTEGRAL CONTROL CONSTRAINT

VALERII PATSKO[1,*], GEORGII TRUBNIKOV[2], ANDREY FEDOTOV[1]

[1]Krasovskii Institute of Mathematics and Mechanics, Ekaterinburg, Russia
[2]Ural Federal University named after the first President of Russia B.N.Yeltsin, Ekaterinburg, Russia

Dedicated to the memory of Professor Josef Shinar

Abstract. A three-dimensional reachable set for a nonlinear controlled object "Dubins car" is investigated. The control is the angular velocity of rotation of the linear velocity vector, which is subjected to an integral quadratic constraint. Based on the Pontryagin maximum principle, a description of the motions generating the boundary of the reachable set is given. If the angles are identified by modulo 2π, then the motions leading to the boundary of the corresponding reachable set represent globally optimal Euler elasticae. Simulation results are presented.

Keywords. Dubins car; Integral control constraint; Three-dimensional reachable set; Pontryagin maximum principle; Euler elasticae; Numerical constructions.

2020 MSC. 33E05, 49K15, 49M05, 93B03, 93C10.

1. INTRODUCTION

This paper is dedicated to the memory of Professor Josef Shinar. The first of the authors of the paper repeatedly discussed with him model formulations of space guidance problems and a possibility of constructing solvability sets in them. Josef Shinar knew and understood such problems better than other specialists in the theory of differential games. In the problem considered in this paper, there is no the second (opposing) player, but the subject of study is very close: the reachable set evolving in time.

By the mathematical "Dubins car"(another name is a "unicycle"), we mean an object moving on a plane with a constant value of linear velocity. Without loss of generality, we assume that the value is equal to 1. The phase state includes two coordinates x, y of the geometric position and the angle φ of the direction of the velocity vector. The angles are measured from the positive direction of the axis x and are not identified by modulo 2π. The scalar control u has the meaning

*Corresponding author.
E-mail address: patsko@imm.uran.ru (V. Patsko), jora_it@mail.ru (G. Trubnikov), andreyfedotov@mail.ru (A. Fedotov).

Received February 11, 2023; Accepted May 14, 2024.

of the instantaneous angular velocity of the turn. The control is restricted on the interval $[0,t_f]$ by an integral quadratic constraint

$$\int_0^{t_f} u^2(t)dt \le \mu \tag{1.1}$$

with a given value $\mu > 0$. The purpose of this paper is to numerically study a three-dimensional reachable set $G(t_f,\mu)$ at time t_f.

Studying the problem of constructing the set $G(t_f,\mu)$, we rely on the experience [8, 9] of analytical description and numerical construction of the reachable set boundary for the case of geometric constraints $|u(t)| \le \mu$. The fundamental difference is that in the case of the geometric constraints, many calculations can be performed explicitly using elementary functions, while in the case of integral constraints, analytical calculations are difficult due to the need to use special elliptic functions. Nevertheless, numerical constructions of the reachable set $G(t_f,\mu)$ are possible, and, in many respects, they are done by an analogy with the case of the geometric constraints. In this regard, in Section 3 following the problem statement, we give a representation of three-dimensional reachable sets under the geometric constraints. Section 8 shows images of three-dimensional reachable sets under the integral constraints, which can be compared with those under the geometric constraints.

The study of the boundary of the three-dimensional reachable set is based on the Pontryagin maximum principle (PMP). However, even before formulating the PMP, we can establish some symmetry properties using only the definition of the reachable set and the specifics of the kinematics of the Dubins car. One of the symmetry properties is that the structure of reachable sets just depends on the value $t_f\mu$. Such a symmetry property allows, having fixed, for example, $t_f = 1$ (or $\mu = 1$), to study the change of the reachable set depending only on μ (respectively, on t_f). Moreover, any φ-section of the three-dimensional reachable set is symmetric with respect to some auxiliary axis X depending on φ. Therefore, when examining a particular φ-section, one can consider only its "half". It also follows from the specifics of the kinematics of the Dubins car that the φ-sections obtained for $\varphi > 0$ are symmetric to the φ-sections for $\varphi < 0$. This property makes it possible to confine ourselves to studying φ-sections only for $\varphi \ge 0$. Symmetry properties are studied in Section 4.

In Section 5, we write down the PMP for open-loop controls $u(\cdot)$ leading to the boundary of the reachable set. Here we use the result from work [4] by M.I. Gusev and I.V. Zykov that the formulation of the PMP is the same as for the problem of minimizing the integral functional

$$J(u(\cdot)) = \int_0^{t_f} u^2(t)dt \tag{1.2}$$

under three-dimensional boundary conditions given at times $t_0 = 0$ and t_f. The only exception is the control $u(t) \equiv 0$. Obviously, it leads to the boundary of the reachable set. Assuming it special, we exclude it from the consideration.

In the formulation of the PMP, the differential equations of the original and adjoint systems, supplemented by the maximum condition, constitute a closed system of the 6th order, the solution to which is completely determined by the three-dimensional initial condition of the original system (we consider it to be zero) and by the assignment of the three-dimensional boundary condition of the adjoint system. Going over the latter boundary condition, we obtain the motions of the initial system, among which there must be motions leading to the boundary of the three-dimensional reachable set. In this case, the controls satisfying the PMP are continuous.

A straight switching line corresponds to each extreme motion. The control changes the sign on this straight line.

The necessary conditions that follow directly from the initial consideration of the PMP are specified in Section 6. The main specification comes down to the fact that any open-loop control leading to the boundary of the reachable set has at most two instants when the sign of the control changes. In the case of two instants t_1 and t_2 $(t_2 > t_1)$ of sign change located on the interval $(0,t_f)$, the inequality $t_2 - t_1 \geq (t_1 - t_0) + (t_f - t_2)$ is true. These statements are easily proved and allow us to formulate Theorem 6.3 that any point on the boundary of the reachable set is attained by a control belonging to one of the 6 types described in the theorem. At the same time, for positive values $\varphi(t_f)$, we can limit ourselves to only 4 types. In Section 7, we write out finite relations for $\varphi(t_f) \geq 0$, based on which we can find all the motions that correspond to the types of controls defining the boundary. The results of the numerical construction of reachable sets $G(t_f,\mu)$ are presented in Section 8.

If it is required to study the reachable set for the case when the angles φ are identified by modulo 2π (i.e., the angles $\varphi \pm 2\pi k$, $k = 0,1,2,...$ are considered equivalent), then it is not difficult to do, provided that we can construct the set $G(t_f,\mu)$ without identifying the angles. The results of numerical constructions under identification by modulo 2π are discussed in Section 9, which gives two examples of such computations.

The extremal motions corresponding to the functional (1.2) under *identification* of the angle φ modulo 2π were classified by L. Euler [3] and are called Euler elasticae. A good historical review on Euler elasticae was done by R. Levien in [7]. The Euler elasticae were studied in detail by Yu.L. Sachkov and A.A. Ardentov in [1, 2] in order to single out globally optimal ones among them. In work [13] of M. I. Zelikin, some properties of generalized Euler elasticae are analyzed in the case when the motion occurs in the multidimensional space R^n, $n \geq 3$. Our results on the selection of globally optimal elasticae, obtained in Section 10, can be considered as additional to the researches of M. I. Zelikin, Yu. L. Sachkov and A. A. Ardentov.

2. Statement of the problem

Let a motion of a controlled object on a plane be described by a system

$$\dot{x} = \cos\varphi, \quad \dot{y} = \sin\varphi, \quad \dot{\varphi} = u. \tag{2.1}$$

Here x,y are the coordinates of the geometric position, φ is the angle of inclination of the velocity vector counted counterclockwise from the positive direction of the axis x. The speed is equal to one. We consider the values of the angle φ on the interval $(-\infty,\infty)$. The initial instant t_0 is equal to zero. Initial values $x(t_0)$, $y(t_0)$, and $\varphi(t_0)$ are also considered zero. Admissible controls are measurable square-integrable functions $u(\cdot)$ satisfying the constraint

$$\int_0^{t_f} u^2(t)dt \leq \mu. \tag{2.2}$$

The reachable set $G(t_f,\mu)$ for $t_f > t_0$ and $\mu > 0$ is the collection of all points $(x,y,\varphi)^\mathsf{T}$, into each of which it is possible to transfer system (2.1) at the time t_f with an admissible control.

Denote by $G_\varphi(t_f,\mu)$ the two-dimensional cross-section (the φ-section) of the set $G(t_f,\mu)$ corresponding to the value φ of the angular coordinate.

Let ∂ be the symbol of the set boundary. If some point $(x,y)^\mathsf{T}$ belongs to $\partial G_\varphi(t_f,\mu)$, then the point $(x,y,\varphi)^\mathsf{T}$ belongs to $\partial G(t_f,\mu)$. The converse, generally speaking, is not true.

It is required to construct and study the three-dimensional reachable set $G(t_f,\mu)$, as well as the motions leading to its boundary.

For the sake of brevity, we put $z=(x,y,\varphi)^{\mathsf{T}}$. We denote by $z^0(t_f)=(t_f,0,0)^{\mathsf{T}}$ the point on $\partial G(t_f,\mu)$ to which the control $u(t)\equiv 0$ leads.

3. KNOWN RESULTS UNDER THE GEOMETRIC CONSTRAINT

In works [8, 9, 10], the reachable set $G(t_f)$ was studied under the geometric constraint on the control. It was shown that the case of asymmetric constraint (with different restrictions on the turning radii to the left and right) reduces to studying the canonical symmetric case $|u(t)|\leq 1$, $t\in[t_0,t_f]$. In this paper, when studying the set $G(t_f,\mu)$ under the integral constraint, we use the ideology of constructing the set $G(t_f)$ under the canonical geometric constraint. In this regard, we give a brief description of the structure of reachable sets under the geometric constraint.

Figure 1 shows the evolution in time of the reachable set $G(t_f)$ from the same perspective. With a certain step along φ, black lines indicate the contours of φ-sections $G_\varphi(t_f)$.

It has been established [8] that in order to construct the boundary of the reachable set, one can restrict oneself to only 6 types of piecewise constant open-loop controls with no more than two switches. The parts of the boundary marked in blue in Fig. 1 are controlled by the following type: on the first time interval, the constant control $+1$ acts, on the second time interval, the zero control is used, on the third interval, the constant control $+1$ acts again. The sum of the lengths of three intervals is equal to t_f; the lengths of the intervals are different for different points of the blue surface. Symmetric to the part of this type is a part of the surface marked in yellow. Here the sequence of control actions has the form -1, 0, -1. The green color shows the part of the boundary, to which the controls in the form $+1$, 0, -1 lead. Symmetric to it, there is the purple part with controls -1, 0, $+1$. The red part corresponds to the controls -1, $+1-1$. Here, the characteristic feature is that the length of the middle time interval is not less than the sum of the lengths of the first and third intervals. Symmetric to the red part is the light blue part, for which the control sequence is $+1$, $-1+1$.

The points of the set $G(t_f)$ with the largest values $|\varphi|$ (i.e., for $\varphi=\pm t_f$) are the points of non-smoothness of the boundary. The connection of the red and blue surfaces is not smooth. The red and blue surfaces do not connect smoothly with the green and purple surfaces.

Between the instants 3π and 4π, there is a small time interval, on which for each instant t_f, the set $G(t_f)$ is not simply connected.

The angle of view for Fig. 1 is chosen so that the rear part of the set $G(t_f)$ is clearly visible. To show the boundary of the set on the front part, we made Fig. 2 (but only for $t_f=1.5\pi$), on which the reachable set is shown from two points of view. On the front side of the set (the upper part of Fig. 2), the junction point of four boundary parts (which are highlighted in blue, green, yellow, and purple colors) corresponds to the control, which is identically equal to zero. Along the four lines of pairwise joining of such surfaces emerging from this point, the boundary of the set $G(t_f)$ is smooth.

When studying the set $G(t_f,\mu)$ with an integral control constraint, many constructions are carried out similarly. We will draw attention to the retention or modification of the properties listed above. Below we establish several additional properties similar to those that were obtained under the geometric constraint.

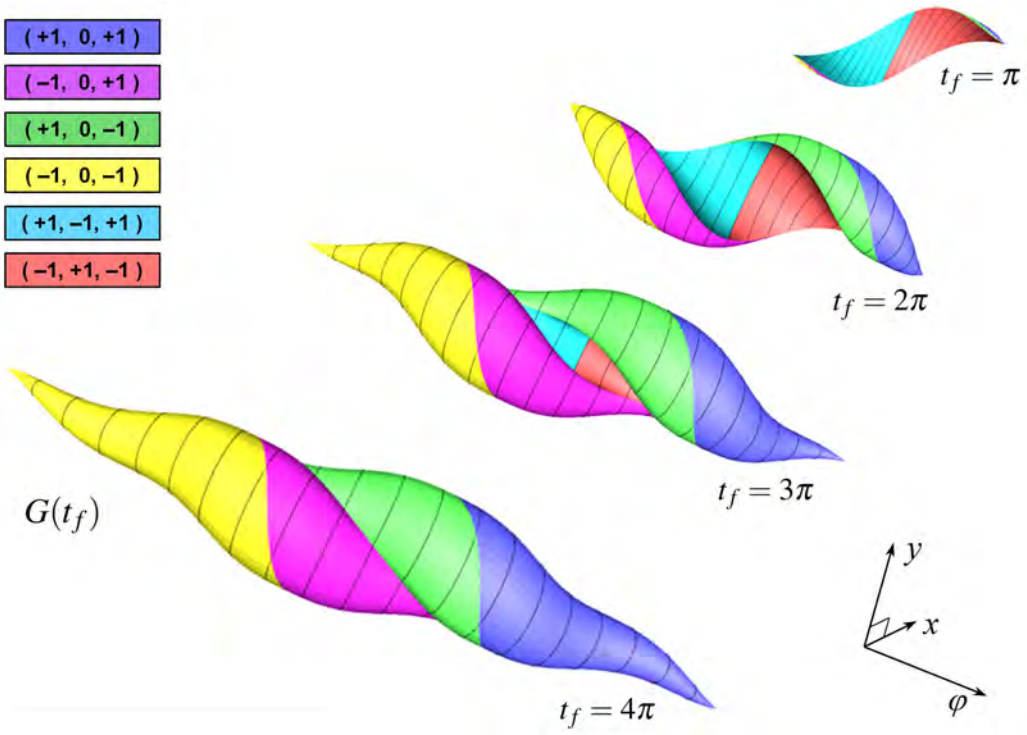

FIGURE 1. Evolution in time of a three-dimensional reachable set $G(t_f)$ under the geometric constraint on the control

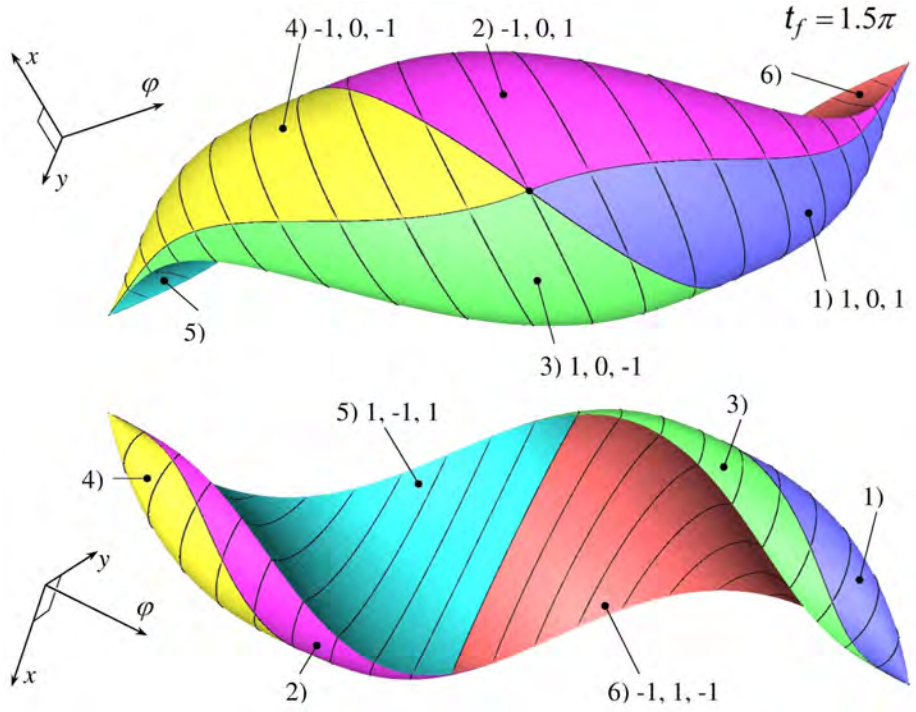

FIGURE 2. Reachable set $G(t_f)$ under the geometric constraint for $t_f = 1.5\pi$ from two points of view

4. Symmetry properties of the three-dimensional reachable set and its φ-sections

4.1. **Range of the set $G(t_f,\mu)$ in φ.** For fixed values t_f and μ, the range of values φ, for which the φ-sections of $G_\varphi(t_f,\mu)$ are not empty, is $\left[-\sqrt{t_f\cdot\mu},\,\sqrt{t_f\cdot\mu}\right]$. Extreme φ-section for $\varphi=\sqrt{t_f\mu}$ (respectively, $\varphi=-\sqrt{t_f\mu}$) consists of a single point generated by the constant control $u(t)\equiv\sqrt{\mu/t_f}$ $(u(t)\equiv-\sqrt{\mu/t_f})$.

We present a schematic proof. Assume that an admissible control $u(\cdot)$ that provides the maximum possible value $\varphi_{\max}$ is not constant. Then there are instants t_1, t_2 and a time interval of length $\triangle t$ such that $t_1+\triangle t$ and $t_2+\triangle t$ belong to $[0,t_f]$, $t_1+\triangle t<t_2$, and also $\int_{t_1}^{t_1+\triangle t}u(t)dt>\int_{t_2}^{t_2+\triangle t}u(t)dt$. We choose $\triangle u>0$ so that

$$\triangle u\cdot\triangle t<\int_{t_1}^{t_1+\triangle t}u(t)dt-\int_{t_2}^{t_2+\triangle t}u(t)dt.$$

Let us introduce a new control $\widetilde{u}(\cdot)$, which differs from $u(\cdot)$ only on the intervals $[t_1,t_1+\triangle t)$ and $[t_2,t_2+\triangle t)$. On the first of these intervals, we put $\widetilde{u}(t)=u(t)-\triangle u$, and on the second interval let $\widetilde{u}(t)=u(t)+\triangle u$. Then $\widetilde{\varphi}(t_f)=\varphi(t_f)$. At the same time,

$$\int_0^{t_f}\widetilde{u}^2(t)dt=\int_0^{t_f}u^2(t)dt+2\triangle u\left(-\int_{t_1}^{t_1+\triangle t}u(t)dt+\int_{t_2}^{t_2+\triangle t}u(t)dt+\triangle u\cdot\triangle t\right)<\int_0^{t_f}u^2(t)dt=\mu.$$

Therefore, for $\widetilde{u}(\cdot)$ the integral control cost will be less than μ. This contradicts the fact that we are considering the maximum possible φ at time t_f under the given constraint μ.

Thus, the last φ-section for $\varphi>0$ is a point. It is generated by the constant control $u(t)\equiv\sqrt{\mu/t_f}$. The corresponding trajectory is an arc of a circumference, a full circumference, or a circumference with an "overlap". The same is true for the extreme φ-section if $\varphi<0$ and $u(t)\equiv-\sqrt{\mu/t_f}$.

4.2. **Symmetry in the space of reachable sets.** The reachable sets under consideration depend on the parameters t_f and μ. Let us show that if $t_f^{(1)}\cdot\mu^{(1)}=t_f^{(2)}\cdot\mu^{(2)}$ (i.e. $\mu^{(1)}/\mu^{(2)}=t_f^{(2)}/t_f^{(1)}=\alpha$), then the φ-sections $G_\varphi(t_f^{(1)},\mu^{(1)})$ and $G_\varphi(t_f^{(2)},\mu^{(2)})$ are rigidly related with each other by the help of the relation $G_\varphi(t_f^{(2)},\mu^{(2)})=\alpha\cdot G_\varphi(t_f^{(1)},\mu^{(1)})$, where the similarity coefficient α does not depend on φ. This symmetry property allows us to restrict ourselves to the study of reachable sets for a fixed value t_f (for example, $t_f=1$), but for different values of μ, or, conversely, for a fixed value μ (for example, for $\mu=1$), but for different t_f.

Lemma 4.1. *Let the values $t_f^{(1)}$, $\mu^{(1)}$ and $t_f^{(2)}$, $\mu^{(2)}$ be such that $t_f^{(1)}\mu^{(1)}=t_f^{(2)}\mu^{(2)}$. Then the domains in φ of the sets $G(t_f^{(1)},\mu^{(1)})$ and $G(t_f^{(2)},\mu^{(2)})$ coincide, and for any φ, the following relation*

$$G_\varphi(t_f^{(2)},\mu^{(2)})=\alpha\,G_\varphi(t_f^{(1)},\mu^{(1)}),\qquad\alpha=t_f^{(2)}/t_f^{(1)}=\mu^{(1)}/\mu^{(2)}$$

holds.

Proof. Since $t_f^{(1)}\mu^{(1)}=t_f^{(2)}\mu^{(2)}$, then the ranges of the sets $G(t_f^{(1)},\mu^{(1)})$ and $G(t_f^{(2)},\mu^{(2)})$ for φ are the same. Consider an arbitrary possible φ.

1) Take an arbitrary point $(x^{(2)},y^{(2)})^{\mathsf{T}} \in G_\varphi(t_f^{(2)},\mu^{(2)})$. Let the control $u^{(2)}(\cdot)$ (defined on $[0,t_f^{(2)}]$ and satisfying the constraint $\int_0^{t_f^{(2)}} (u^{(2)}(s))^2 ds \le \mu^{(2)}$) lead to it. Let us create the control

$$u^{(1)}(t) = \alpha u^{(2)}(\alpha t),\ t \in [0,t_f^{(1)}].$$

We get $\alpha t \in [0,\alpha t_f^{(1)}] = [0,t_f^{(2)}]$.

We fix an arbitrary instant $\widetilde{t} \in [0,t_f^{(1)}]$. Let us assign to it the instant $\widetilde{s} = \alpha\widetilde{t}$. We have

$$\varphi^{(2)}(\widetilde{s}) = \int_0^{\widetilde{s}} u^{(2)}(s)ds.$$

The control $u^{(1)}(\cdot)$ gives

$$\varphi^{(1)}(\widetilde{t}) = \int_0^{\widetilde{t}} u^{(1)}(t)dt = \int_0^{\widetilde{t}} \alpha u^{(2)}(\alpha t)dt.$$

Applying the relation $s=\alpha t$, we get $ds=\alpha dt$ and hence

$$\varphi^{(1)}(\widetilde{t}) = \int_0^{\widetilde{s}} u^{(2)}(s)ds = \varphi^{(2)}(\widetilde{s}).$$

In particular, $\varphi^{(1)}(t_f^{(1)}) = \varphi^{(2)}(t_f^{(2)}) = \varphi$.

We calculate the integral control cost for $u^{(1)}(\cdot)$:

$$\int_0^{t_f^{(1)}} (u^{(1)}(t))^2 dt = \int_0^{t_f^{(1)}} \alpha^2 (u^{(2)}(\alpha t))^2 dt = \alpha \int_0^{t_f^{(2)}} (u^{(2)}(s))^2 ds \le \alpha\mu^{(2)} = \frac{\mu^{(2)} t_f^{(2)}}{t_f^{(1)}} = \mu^{(1)}.$$

For the value $x^{(1)}(t_f^{(1)})$, we get

$$x^{(1)}(t_f^{(1)}) = \int_0^{t_f^{(1)}} \cos(\varphi^{(1)}(t))dt = \frac{1}{\alpha}\int_0^{t_f^{(1)}} \alpha\cos(\varphi^{(2)}(\alpha t))dt = \frac{1}{\alpha}\int_0^{t_f^{(2)}} \cos(\varphi^{(2)}(s))ds = \frac{1}{\alpha}x^{(2)}(t_f^{(2)}).$$

Similarly, $y^{(1)}(t_f^{(1)}) = \frac{1}{\alpha}y^{(2)}(t_f^{(2)})$.

Therefore,

$$G_\varphi(t_f^{(1)},\mu^{(1)}) \supset \frac{1}{\alpha} G_\varphi(t_f^{(2)},\mu^{(2)}). \tag{4.1}$$

2) Take the point $(x^{(1)},y^{(1)})^{\mathsf{T}} \in G_\varphi(t_f^{(1)},\mu^{(1)})$. Let the control $u^{(1)}(\cdot)$ (defined on $[0,t_f^{(1)}]$ and satisfying the constraint $\int_0^{t_f^{(1)}} (u^{(1)}(t))^2 dt \le \mu^{(1)}$) lead to it. Let us create the control

$$u^{(2)}(s) = \frac{1}{\alpha}u^{(1)}\Big(\frac{s}{\alpha}\Big), \quad s \in [0,t_f^{(2)}].$$

Making the calculations similar to the item 1), we obtain

$$\alpha G_\varphi(t_f^{(1)},\mu^{(1)}) \subset G_\varphi(t_f^{(2)},\mu^{(2)}). \tag{4.2}$$

From (4.1), (4.2), it follows

$$\alpha G_\varphi(t_f^{(1)},\mu^{(1)}) = G_\varphi(t_f^{(2)},\mu^{(2)}).$$

□

4.3. **Symmetry of cross-sections of the set $G(t_f,\mu)$ along the angular coordinate.** Let $t\to u(t)$ be an admissible control leading at the instant t_f to some point $z(t_f)$ of the set $G(t_f,\mu)$. We introduce a "reverse" control $u^{\#}(t)=u(t_f-t),\ \ t\in[0,t_f]$. Obviously, the new control will be admissible with the same value of the integral of the squared control.

Consider the motion $t\to z^{\#}(t)=\left(x^{\#}(t),y^{\#}(t),\varphi^{\#}(t)\right)^{\mathsf{T}}$ by virtue of the control $u^{\#}(\cdot)$. We have

$$\varphi(t)=\int_0^t u(\tau)d\tau,\qquad \varphi^{\#}(t)=\int_0^t u^{\#}(\tau)d\tau=\int_0^t u(t_f-\tau)d\tau=\int_{t_f-t}^{t_f} u(\tau)d\tau. \tag{4.3}$$

Therefore, $\varphi^{\#}(t_f)=\varphi(t_f)$.

We draw the auxiliary axis X through the origin of the system x,y at the angle $\varphi(t_f)/2$ with respect to the direction of the axis x (see Fig. 3). Assume that the axis Y is orthogonal to the axis X. By the symbols $\left(X(t_f),Y(t_f)\right)^{\mathsf{T}}$ and $\left(X^{\#}(t_f),Y^{\#}(t_f)\right)^{\mathsf{T}}$, we denote the positions of the points $\left(x(t_f),y(t_f)\right)^{\mathsf{T}}$ and $\left(x^{\#}(t_f),y^{\#}(t_f)\right)^{\mathsf{T}}$ in the auxiliary coordinate system X,Y.

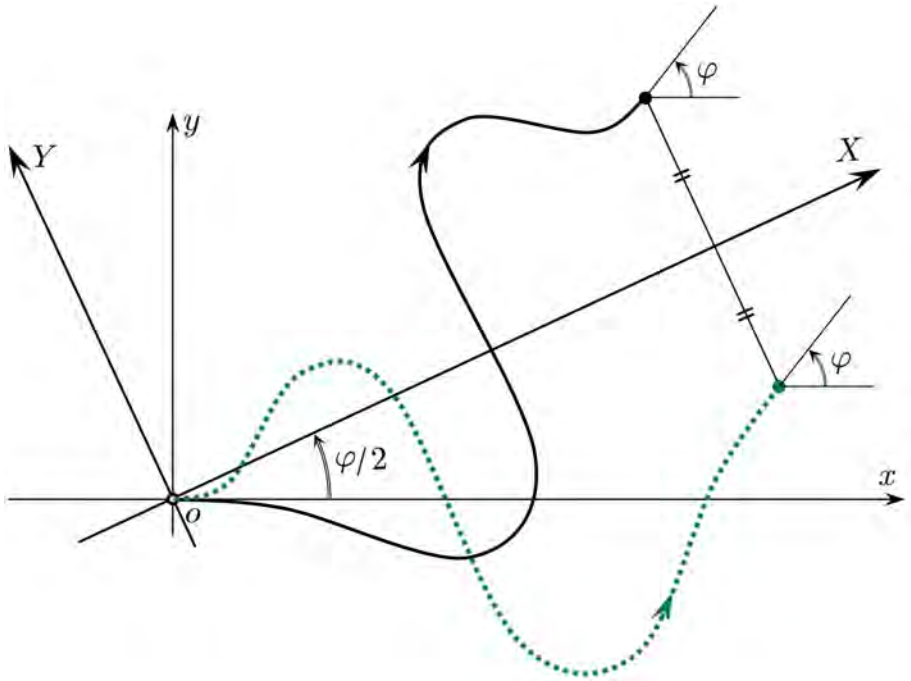

FIGURE 3. Auxiliary coordinate system. Direct and reverse motions

Lemma 4.2. *The relations $X^{\#}(t_f)=X(t_f)$, $Y^{\#}(t_f)=-Y(t_f)$ are valid.*

Proof. From formulas (4.3), we get $\varphi^{\#}(t)=\varphi(t_f)-\varphi(t_f-t)$. Let us introduce the angles counted from the axis X:

$$\varphi_X(t)=\varphi(t)-\frac{\varphi(t_f)}{2},$$

$$\varphi_X^{\#}(t)=\varphi^{\#}(t)-\frac{\varphi(t_f)}{2}=\varphi(t_f)-\varphi(t_f-t)-\frac{\varphi(t_f)}{2}=-\left(\varphi(t_f-t)-\frac{\varphi(t_f)}{2}\right).$$

Then

$$Y(t_f)=\int_0^{t_f}\sin\left(\varphi(t)-\frac{\varphi(t_f)}{2}\right)dt,$$

$$Y^{\#}(t_f)=\int_0^{t_f}\sin\left[-\left(\varphi(t_f-t)-\frac{\varphi(t_f)}{2}\right)\right]dt=-\int_0^{t_f}\sin\left(\varphi(s)-\frac{\varphi(t_f)}{2}\right)ds=-Y(t_f).$$

Replacing sin in the integrals with cos and taking into account that cos is an even function, we get $X^{\#}(t_f)=X(t_f)$. □

It follows from Lemma 4.2 that any φ-section $G_\varphi(t_f,\mu)$ is symmetric with respect to the axis X of the auxiliary coordinate system. Note that this property of symmetry relative to the axis X was also established [9] under the geometric constraint on the control.

4.4. **Symmetry of φ-sections for $\varphi>0$ and $\varphi<0$.** The problem under consideration also has a symmetry of φ-sections for positive and negative values φ. Namely, the φ-section $G_{\overline{\varphi}}(t_f,\mu)$ for $\overline{\varphi}<0$ is related to the φ-section $G_{\widetilde{\varphi}}(t_f,\mu)$, where $\widetilde{\varphi}=-\overline{\varphi}$, by mirror reflection about the axis x. It follows from the fact that the motions of system (2.1) from the initial zero point $z(t_0)$ due to the controls $\overline{u}(\cdot)$ and $\widetilde{u}(\cdot)=-\overline{u}(\cdot)$ are related by $\overline{x}(\cdot)=\widetilde{x}(\cdot)$, $\overline{y}(\cdot)=-\widetilde{y}(\cdot)$, $\overline{\varphi}(\cdot)=-\widetilde{\varphi}(\cdot)$.

This fact also took place for the geometric constraint $|u(t)|\leq 1$.

5. Pontryagin maximum principle

It follows from the general results of mathematical control theory that the set $G(t_f,\mu)$ is closed and bounded (see, for example, [4, 5, 6]). In [4], it is shown that for any point $z(t_f)\in\partial G(t_f,\mu)$ such that $z(t_f)\neq z^0(t_f)$, there is the Pontryagin maximum principle (PMP) written for the problem of minimizing functional (1.2) on the motions of system (2.1) with fixed boundary conditions $z(t_0)=0$ and $z(t_f)$. Herewith, the minimum of the functional is equal to μ.

1) Let us write the PMP relations for the functional (1.2) minimization problem with fixed boundary conditions in system (2.1) (see, for example, [13, 1, 4]). Let $u(\cdot)$ be an admissible control not identically zero, and $(x(\cdot),y(\cdot),\varphi(\cdot))^{\mathsf{T}}$ is the corresponding motion of system (2.1) on the interval $[t_0,t_f]$. The differential equations of the adjoint system have the form

$$\dot{\psi}_1=0,\qquad \dot{\psi}_2=0,\qquad \dot{\psi}_3=\psi_1\sin\varphi(t)-\psi_2\cos\varphi(t). \tag{5.1}$$

The PMP means that if $u(\cdot)$ is a minimizing control, then there is a nonzero solution $(\psi_1(\cdot),\psi_2(\cdot),\psi_3(\cdot))^{\mathsf{T}}$ of system (5.1), for which the equality

$$u(t)=\psi_3(t)/2 \tag{5.2}$$

is fulfilled. In what follows, a control that satisfies the PMP is assumed to be continuous.

The functions $\psi_1(\cdot)$ and $\psi_2(\cdot)$ are constants. Let us denote them ψ_1 and ψ_2. If $\psi_1=0$ and $\psi_2=0$, then $\psi_3(t)\equiv\text{const}\neq 0$. Therefore, in this case $u(t)\equiv\text{const}=\pm\sqrt{\mu/t_f}$. Such constant controls determine the extreme one-point φ-sections $G_\varphi(t_f,\mu)$ for $\varphi=\pm\sqrt{t_f\mu}$.

Let now at least one of the numbers ψ_1, ψ_2 is not equal to zero. Based on (2.1) and (5.1), we can write the expression $\psi_3(t) = \psi_1 y(t) - \psi_2 x(t) + C$. It implies that $\psi_3(t) = 0$ if and only if the point $(x(t), y(t))^{\mathsf{T}}$ of the geometric position at the instant t satisfies the equation of a straight line

$$\psi_1 y - \psi_2 x + C = 0. \tag{5.3}$$

Straight switching line (5.3) is not universal: when the control that satisfies the PMP is changed, the switching line also changes. In the sequel, instead of "straight switching line", we will write SSL.

Complementing systems (2.1) and (5.1) with relation (5.2), we arrive at a closed system of differential equations, for which the standard conditions of the theorems of existence and uniqueness of the solution are satisfied. Therefore, in particular, there cannot be motions on the plane x, y that would approach the SSL tangentially in a finite time. Likewise, there cannot be motions that leave the SSL after some movement along it. It is only possible to cross the SSL under a non-zero angle, or to leave it at the initial instant (respectively, to entry at the last instant) with a non-zero angle. Considering in addition to the fixed initial condition $z(t_0) = 0$ the values ψ_1, ψ_2, and $\psi_3(t_0)$, we obtain a collection of motions $t \to z(t)$, among which there must be all the motions leading to $\partial G(t_f)$.

2) Taking into account equality (5.2), we write the equations for $\dot{\varphi}$ and $\dot{\psi}_3$ (with the stipulated constants ψ_1 and ψ_2) in the form of the single equation of the second order:

$$\ddot{\varphi}(t) = \rho \sin(\varphi(t) - \beta). \tag{5.4}$$

Here, ρ is the length of the vector with the components $\psi_1/2$, $\psi_2/2$, and β is the angle slope of this vector counted counterclockwise from the axis x. Thus, enumeration of the constants ψ_1, ψ_2, $\psi_3(0)$ can be replaced by enumeration of the constants ρ, β and $\dot{\varphi}(0) = \psi_3(0)/2$.

Multiplying relation (5.4) by $2\dot{\varphi}(t)$ (by analogy with [13], p. 282), we have

$$\frac{d\,(\dot{\varphi}(t))^2}{dt} = 2\dot{\varphi}(t)\ddot{\varphi}(t) = 2\dot{\varphi}(t)\rho \sin(\varphi(t) - \beta).$$

Therefore,

$$(\dot{\varphi}(t))^2 = c_* - 2\rho \cos(\varphi(t) - \beta). \tag{5.5}$$

For $\dot{\varphi}(t) \neq 0$, we get

$$\dot{\varphi}(t) = \pm\sqrt{c_* - 2\rho \cos(\varphi(t) - \beta)}. \tag{5.6}$$

We use this formula on the intervals of the motion where $\dot{\varphi}(t) \neq 0$. The sign "+" corresponds to the control $u(t) > 0$, the sign "−" means that $u(t) < 0$. Bearing in mind expression (5.3) for SSL and considering the equality $\psi_3(t)/2 = \dot{\varphi}(t)$, we get that the sign "+" in front of the root means a motion in one half-plane defined by the SSL, and the sign "−" corresponds to a motion in the other half-plane. Let us agree to choose the direction of the SSL so that the half-plane, where $u > 0$, lies on the left, and the half-plane with $u < 0$ on the right.

The angle β is equal to the angle (counted counterclockwise) between the direction of the axis x and the direction of the SSL. It can be shown that the constants C in (5.3) and c_* in (5.5) are related by the equality $c_* = 2\rho\cos\beta + C^2/4$. If at some instant t the point $(x(t), y(t))^{\mathsf{T}}$ lies on SSL, then

$$c_* = 2\rho\cos\beta'. \tag{5.7}$$

Here $\beta' = \beta - \varphi(t)$ is the angle of inclination of the velocity vector of system (1.1) at the instant t with respect to the direction of SSL (counted counterclockwise from the velocity vector direction).

From (5.6), we have

$$dt = \frac{d\varphi}{\pm\sqrt{c_* - 2\rho\cos(\varphi - \beta)}}. \tag{5.8}$$

Formula (5.8) allows one to replace an integration over t with an integration over φ in half-planes with a constant control sign.

3) Except for the special motion under $u(\cdot)\equiv 0$, only the following two variants of the relative disposition of the motion trajectory $(x(\cdot), y(\cdot))^{\mathsf{T}}$ and the straight switching line are possible (Fig. 4).

3.1) The trajectory does not cross the SSL (Fig. 4a). In this case, the function $\psi_3(\cdot)$ has the same sign on the entire interval $[t_0, t_f]$.

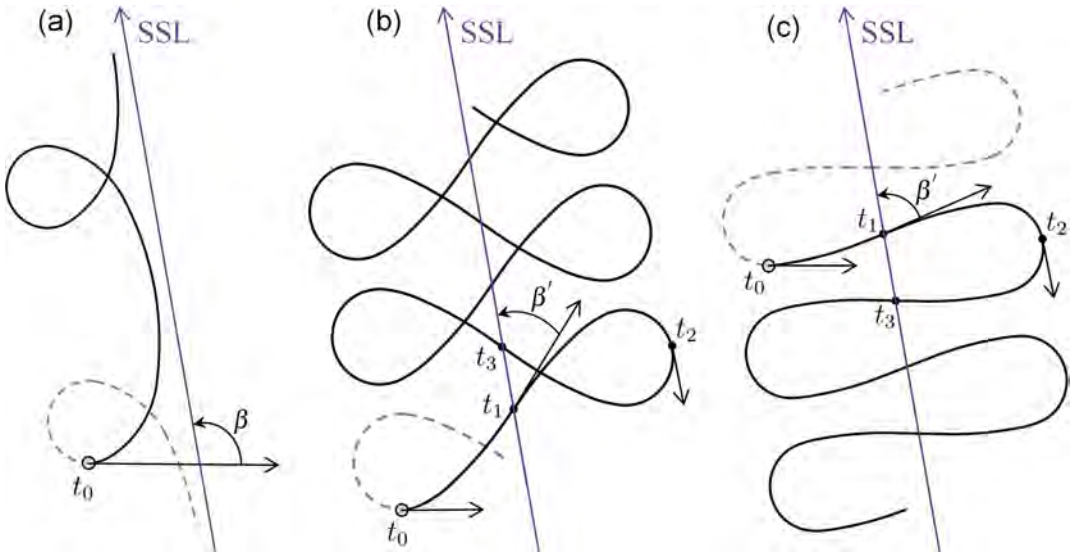

FIGURE 4. Mutual arrangement of the trajectory $(x(\cdot), y(\cdot))^{\mathsf{T}}$ and the straight switching line

3.2) The trajectory intersects the SSL at some instant t_1 under a non-zero angle. For definiteness, consider the changing of the sign of the control from "+" to "−" (Figs. 4b and 4c; on the first of them, the trajectory has self-intersection points, on the second one, there are none). The intersection angle β' is equal to $\beta - \varphi(t_1)$. We have $\beta' \in (0, \pi)$.

Then for $t > t_1$, the angle $\varphi(t)$ decreases and at some instant t_2 the direction of the velocity vector becomes opposite to the direction of the SSL. Herewith $\varphi(t_2) = \varphi(t_1) - \pi + \beta'$ (Figs. 4b and 4c). After that, up to the instant $t_3 = 2t_2 - t_1$, the motion proceeds symmetrically

to the one constructed on the interval from t_1 to t_2 (because the value of the control is determined only by the distance from the current point and the SSL). At the instant t_3, the motion hits the SSL and the equality $\varphi(t_3) = \varphi(t_2) - \pi + \beta'$ is fulfilled. In total, on the interval from t_1 to t_3, the value of the accumulated angle is negative and equals modulo $2\pi - 2\beta'$. After switching the control sign from "+" to "−" (if the time t_f has not yet been reached), we have a motion with control sign "+", which is centrally symmetrical to the previous one with the center at the second point of control sign change.

Thus, the accumulated angle on each interval of control sign constancy does not exceed 2π, and motions between adjacent areas of constancy of the control sign are symmetric to each other. It follows from the symmetry property that the time between adjacent switching instants is the same. Therefore, the function $\psi_3(\cdot)$ changes sign on the interval $[t_0, t_f]$ a finite number of times.

The foregoing allows us to formulate the following assertion.

Proposition 5.1. *Let the motion $z(\cdot)$ of system (2.1) on the interval $[t_0, t_f]$ be generated by a continuous control $u(\cdot)$ (not equal to zero identically) and the PMP is satisfied. Then the control $u(\cdot)$ changes sign at most a finite number of times. In addition:*

a) the points of the geometric position of system (2.1) on the plane x, y at the instants of sign change of the control $u(\cdot)$ lie on the SSL;

b) if $z(\cdot)$ is such that the motion $(x(\cdot), y(\cdot))^{\mathsf{T}}$ intersects the SSL at least three times, then the interval between neighboring crossings of the SSL is the same; the corresponding increment of the angle modulo is also the same;

c) if $z(\cdot)$ is such that the motion $(x(\cdot), y(\cdot))^{\mathsf{T}}$ intersects the SSL at least once, then the accumulated angle modulo does not exceed 2π on each interval of control sign constancy;

d) if $z(\cdot)$ is such that the motion $(x(\cdot), y(\cdot))^{\mathsf{T}}$ crosses the SSL twice at some times t_1 and $t_2 > t_1$, then the inequality $(t_1 - t_0) + (t_f - t_2) > t_2 - t_1$ is equivalent to the inequality $|\varphi(t_1) - \varphi(t_0)| + |\varphi(t_f) - \varphi(t_2)| > |\varphi(t_2) - \varphi(t_1)|$.

4) As it was said in the item 1), the maximum principle made it possible to write down the system of differential equations (2.1), (5.1) closed by (5.2). In this system, the initial conditions $x(0)$, $y(0)$, and $\varphi(0)$ are taken equal to zero. Going through the values ψ_1, ψ_2, $\psi_3(0)$, we obtain a set of motions $x(\cdot), y(\cdot), \varphi(\cdot)$, each of which is defined on an infinite time interval. For any fixed instant t_f and any boundary condition $x(t_f), y(t_f), \varphi(t_f)$, the optimal motion delivering a minimum equal to μ to the integral functional is among the specified set of motions considered on the interval $[t_0, t_f]$.

The resulting set of motions coincides with the one that was classified by L. Euler in book [3, Addition 1]. Later extremal motions were called Euler elasticae. Euler elasticae that are globally optimal in the sense of the functional (1.2) will be discussed in Section 10. It should be kept in mind that in Euler's setting, the angles given at the time t_f are *identified* by modulo 2π. That is why not every control leading to the boundary of the reachable set $G(t_f, \mu)$ is globally optimal (with the value of the optimum equal to μ) in the functional (1.2) minimization problem when identifying angles.

In the next section, having fixed an arbitrary value $\mu > 0$, we will reveal some additional properties of motions (from the considered set) that lead to the reachable set boundary.

6. Refinement of necessary conditions for controls leading to the boundary of the reachable set

In the statements below, it is assumed that the consumption of the integral resource on the admissible control under consideration is equal to μ.

Lemma 6.1. *Let the motion $z(\cdot)$ of system (2.1) on the interval $[t_0,t_f]$ be generated by a continuous control $u(\cdot)$ satisfying the PMP with two instants t_1, t_2 of control sign change, where $t_0<t_1<t_2<t_f$. Assume that*

$$(t_1-t_0)+(t_f-t_2)>(t_2-t_1). \tag{6.1}$$

Then $z(t_f)\in \operatorname{int} G(t_f,\mu)$.

Proof. Without losing the generality, we accept the following sequence of control $u(\cdot)$ signs: $-,+,-$. In this case, by Proposition 5.1d, the inequality (6.1) is equivalent to the inequality $-(\varphi(t_1)-\varphi(t_0))-(\varphi(t_f)-\varphi(t_2))>\varphi(t_2)-\varphi(t_1)$.

Assume by contradiction that $z(t_f)\in\partial G(t_f)$. Then any control leading to this point satisfies the PMP. We choose instants $\overline{t}\in(t_0,t_1)$ and $\widehat{t}\in(t_2,t_f)$ so that the equality

$$-(\varphi(t_1)-\varphi(\overline{t}))-(\varphi(\widehat{t})-\varphi(t_2))=\varphi(t_2)-\varphi(t_1)$$

holds. The possibility of such a choice follows from the continuity of $\varphi(t)$. We have $\varphi(\overline{t})=\varphi(\widehat{t})$.

Consider the reverse control $u^{\#}(t)=u(\widehat{t}-t)$ on the interval $[\overline{t},\widehat{t}]$. Replacing the initial condition $z(t_0)=0$ in Lemma 4.2 with $z(\overline{t})$ and taking into account the equality $\varphi(\overline{t})=\varphi(\widehat{t})$, we get $\big(X(\widehat{t}),Y(\widehat{t})\big)^{\mathsf{T}}=\big(X^{\#}(\widehat{t}),-Y^{\#}(\widehat{t})\big)^{\mathsf{T}}$. The constructions are explained in Fig. 5, where the axis X from Lemma 4.2 is denoted by $\overline{X}$.

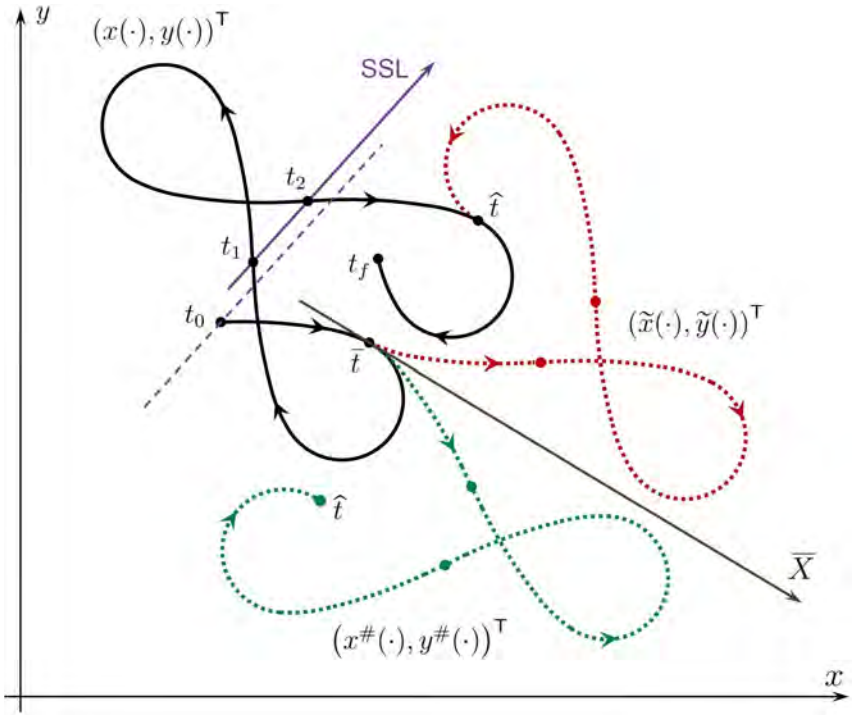

FIGURE 5. Explanation to the proof of Lemma 6.1. The solid line is the initial motion $(x(\cdot),y(\cdot))^{\mathsf{T}}$. The green dotted line is the reverse motion $\big(x^{\#}(\cdot),y^{\#}(\cdot)\big)^{\mathsf{T}}$ on $[\overline{t},\widehat{t}]$. The red dotted line is the auxiliary motion $(\widetilde{x}(\cdot),\widetilde{y}(\cdot))^{\mathsf{T}}$ on $[\overline{t},\widehat{t}]$

Let take the control $\widetilde{u}(t) = -u^{\#}(t)$, $t \in [\bar{t}, \widehat{t}\,]$. For the corresponding auxiliary motion (red dotted line in Fig. 5) starting from the point $z(\bar{t}\,)$, we get $\widetilde{z}(\widehat{t}\,) = z(\widehat{t}\,)$. Let us extend the control $\widetilde{u}(\cdot)$ and the corresponding motion $\widetilde{z}(\cdot)$ onto the interval $[t_0, t_f]$ setting $\widetilde{u}(t) = u(t)$ as $t \in [t_0, \bar{t}\,) \cup (\widehat{t}\,, t_f]$. The integral control cost for $\widetilde{u}(\cdot)$ on $[t_0, t_f]$ coincides with the control cost for $u(\cdot)$. We have $\widetilde{z}(t_f) = z(t_f)$. Therefore, the control $\widetilde{u}(\cdot)$ also leads to $\partial G(t_f, \mu)$. At that, $\widetilde{u}(\bar{t} - 0) < 0$ and $\widetilde{u}(\bar{t} + 0) = -u^{\#}(\bar{t} + 0) = -u(\widehat{t} - 0) > 0$. Similarly, $\widetilde{u}(\widehat{t} - 0) < 0$ and $\widetilde{u}(\widehat{t} + 0) = -u(\widehat{t} + 0) > 0$. Thus, the control $\widetilde{u}(\cdot)$, considered on $[t_0, t_f]$, is discontinuous at the instants $\bar{t}, \widehat{t}$ and, therefore, does not satisfy the PMP. □

Lemma 6.2. *Let the motion $z(\cdot)$ of system (2.1) on the interval $[t_0, t_f]$ be generated by a continuous control $u(\cdot)$ that satisfies the PMP with three instants t_1, t_2, t_3 of the control sign change, and besides $t_0 < t_1 < t_2 < t_3 < t_f$. Then $z(t_f) \in \operatorname{int} G(t_f, \mu)$.*

Proof. By Proposition 5.1b, we have $t_2 - t_1 = t_3 - t_2$. Therefore, on the interval $[t_1, t_f]$, the conditions of Lemma 6.1 are satisfied with the initial position and initial angle specified at the instant t_1, as well as with the instants t_2 and t_3 of control sign change (with an integral constraint equal to the difference between the original constraint μ and the integral of the control square on $[t_0, t_1]$). Therefore, the considered motion comes at the instant t_f to the interior of the reachable set constructed on the interval $[t_1, t_f]$ from the initial state $z(t_1)$. Hence $z(t_f) \in \operatorname{int} G(t_f, \mu)$. □

Let us introduce the types of continuous controls $u(\cdot)$ with at most two instants of change of the control sign. The type U_1 is characterized by the fact that $u(t) > 0$ on the entire interval $[t_0, t_f]$. Similarly, we define the type U_4 with the positive control replaced by a negative one. The type U_3 has one instant of changing sign of the control, while at the beginning there is a sign "+", then "−". The type U_2 also has one instant of sign change, but only from "−" to "+". We will also include to U_3 (respectively, to U_2) such controls for which $u(t) > 0$ (respectively, $u(t) < 0$), $t \in (t_0, t_f)$, and at least one of the values $u(t_0)$, $u(t_f)$ is zero. The type U_5 is given by two sign change instants and a sequence $+, -, +$. The type U_6 has two instants of changing the control sign and the sequence $-, +, -$.

Theorem 6.3. *For any point $z(t_f) \neq z^0(t_f)$ on $\partial G(t_f, \mu)$, there is a continuous control, leading to this point, that satisfies the PMP and belongs to one of the types $U_1 - U_6$. There are no other control variants leading to the boundary.*

If $\varphi(t_f) > 0$, then we leave only four types in the list of six types: U_1, U_2, U_3, U_6. In the case $\varphi(t_f) < 0$, we restrict ourselves to four types U_2, U_3, U_4, U_5. If $\varphi(t_f) = 0$, we leave the types U_2, U_3, U_5, U_6; in this case, controls of the types U_5 and U_6 generate the same set of points.

Proof. For any point $z(t_f) \neq z^0(t_f)$ on $\partial G(t_f, \mu)$, there is a control (leading to this point) that satisfies the PMP. By the virtue of Proposition 5.1, it has at most a finite number of sign change instants.

Assume by contradiction that on $\partial G(t_f, \mu)$ there is a point $\widehat{z}$, the transferring to which is possible using a control with three or more sign changes. If there are several such controls, then we take the control $u^{\diamond}(\cdot)$ with the least number of sign change. The motion generated by it, we denote by $z^{\diamond}(\cdot)$. Let us consider the motion of $z^{\diamond}(\cdot)$ on the last four intervals of constant control sign. By virtue of Lemma 6.2, we obtain $z^{\diamond}(t_f) \in \operatorname{int} G(t_f, \mu)$.

Thus, to any point $z(t_f) \neq z^0(t_f)$ on $\partial G(t_f, \mu)$, we can pass using a control related to one of the types $U_1 - U_6$. Taking Lemmas 4.2 and 6.1 into account, this fact can be refined in the following way, depending on the sign of the angle φ for the point under consideration $z(t_f) = \big(x(t_f), y(t_f), \varphi(t_f)\big)^{\mathsf{T}}$.

Any control of the type U_1 leads to a point with $\varphi(t_f) > 0$. For controls of the type U_4, we have $\varphi(t_f) < 0$. Therefore, the types U_1 and U_4 are excluded for $\varphi(t_f) = 0$. By virtue of Lemma 4.2, the controls U_5 and U_6 for $\varphi(t_f) = 0$ generate the same set of points $\big(x(t_f), y(t_f)\big)^{\mathsf{T}}$.

Let $\varphi(t_f) > 0$. Controls of the type U_4 are excluded. Controls of the type U_5 are also excluded, since by virtue of Lemma 6.1, such controls lead to the interior of the reachable set.

The case of $\varphi(t_f) < 0$ is treated similarly. Here we also get four control variants: U_2, U_3, U_4, U_5. □

The types of controls $U_1 - U_6$ are similar to those types that were considered in [8, 9] for the geometric constraint on control. The difference is that in the problem under the integral constraint, when formally describing the types $U_1 - U_6$, there are no intervals with zero control. The above mentioned Theorem 6.3 is also similar to Theorem 1 from [8] and Theorem 1 from [10]. A slight difference is that, under the integral constraint, the controls $U_1 - U_6$ exhaust the motions leading to the boundary.

Next, we use Theorem 6.3 to describe the motions leading to the boundary of the reachable set. The reachable set will be considered as a collection of cross-sections along φ (φ-sections). We restrict ourselves to the values φ from the interval $[0, \sqrt{t_f \mu})$. The φ-section for $\varphi = \sqrt{t_f \mu}$ is the single point. For $\varphi \in [-\sqrt{t_f \mu}, 0)$, the φ-sections are obtained from the symmetry property.

7. Calculation relations for motions with controls of U_1, U_2, U_3, and U_6 types

We fix the values t_f and μ. Let us assume that $\varphi = \varphi(t_f) \in [0, \sqrt{t_f \mu})$. To describe the curves from which the boundary of the φ-section is formed, we will use the curves A_1, A_2, A_3, and A_6, which are generated by controls of the types U_1, U_2, U_3, and U_6.

7.1. **Curve A_1.** Such a curve consists of points, to each of which a positive control leads. We have $\varphi(t_f) > 0$. The following relations are valid:

$$t_f = \int_0^{\varphi(t_f)} \frac{d\varphi}{\sqrt{c_* - 2\rho \cos(\varphi - \beta_1)}}, \tag{7.1}$$

$$\mu = \int_0^{\varphi(t_f)} \sqrt{c_* - 2\rho \cos(\varphi - \beta_1)}\; d\varphi. \tag{7.2}$$

Here, β_1 is the angle measured from the axis x (along which the velocity vector is directed at the initial instant) counterclockwise up to the direction of the SSL. In section 5, this angle was indicated by β.

1) The integrals in relations (7.1), (7.2) are reduced by a simple transformation to elliptic integrals of the first and second kind [12].

We will present such a transformation for the integral in (7.1). Let us make a change of variables $\varphi-\beta_1=2\gamma-\pi$. Relation (7.1) takes the form

$$t_f \;=\; 2\int_0^{\left(\varphi(t_f)-\beta_1+\pi\right)/2}\frac{d\gamma}{\sqrt{c_*+2\rho\cos 2\gamma}} \;-\; 2\int_0^{(-\beta_1+\pi)/2}\frac{d\gamma}{\sqrt{c_*+2\rho\cos 2\gamma}}.$$

Let us transform the radical expression:

$$c_*+2\rho\cos 2\gamma = c_*+2\rho\left(1-2\sin^2\gamma\right) = c_*+2\rho-4\rho\sin^2\gamma = (c_*+2\rho)\left(1-\frac{4\rho}{c_*+2\rho}\sin^2\gamma\right).$$

Considering that $c_*-2\rho\cos(\varphi-\beta_1)\geq 0$, we set

$$k^2=\frac{4\rho}{c_*+2\rho}>0. \tag{7.3}$$

From here,

$$t_f \;=\; \frac{2}{\sqrt{c_*+2\rho}}\left(\int_0^{\left(\varphi(t_f)-\beta_1+\pi\right)/2}\frac{d\gamma}{\sqrt{1-k^2\sin^2\gamma}} \;-\; \int_0^{(-\beta_1+\pi)/2}\frac{d\gamma}{\sqrt{1-k^2\sin^2\gamma}}\right).$$

On the right side of this expression, we have two classical elliptic integrals of the first kind [12].

Similarly, the right side of formula (7.2) reduces to the elliptic integrals of the second kind:

$$\mu=2\sqrt{c_*+2\rho}\left(\int_0^{\left(\varphi(t_f)-\beta_1+\pi\right)/2}\sqrt{1-k^2\sin^2\gamma}\,d\gamma-\int_0^{(-\beta_1+\pi)/2}\sqrt{1-k^2\sin^2\gamma}\,d\gamma\right). \tag{7.4}$$

2) Writing the product $t_f\cdot\mu$, we get

$$t_f\cdot\mu \;=\; 4\left(\int_{(-\beta_1+\pi)/2}^{\left(\varphi(t_f)-\beta_1+\pi\right)/2}\frac{d\gamma}{\sqrt{1-k^2\sin^2\gamma}}\right)\cdot\left(\int_{(-\beta_1+\pi)/2}^{\left(\varphi(t_f)-\beta_1+\pi\right)/2}\sqrt{1-k^2\sin^2\gamma}\,d\gamma\right). \tag{7.5}$$

Consider (7.5) as an equation with respect to k. Since t_f, μ, and $\varphi(t_f)$ are fixed, the solution depends only on β_1. Having determined k from (7.5), we find $(c_*+2\rho)$ from (7.4). The getting value is substituted into formula (7.3) for k^2. As a result, we find the values ρ and c_* (depending on β_1).

Next, we integrate the first two equations of system (2.1) on $[0,t_f]$, taking into account (5.6). We get a motion on the plane x,y, the end of which will be denoted by $A_1(\beta_1)$.

3) If $\beta_1=\varphi(t_f)/2$, then the corresponding motion comes onto the axis X. In this case, the direction of the SSL coincides with the direction of the axis X, and the motion under consideration lies strictly to the left of the SSL. The construction of the curve A_1 is convenient to start from this very point, by going over β_1 in the range $\left[\frac{\varphi(t_f)}{2},\,\frac{\varphi(t_f)}{2}+\pi\right]$.

We increment β_1 from the value $\varphi(t_f)/2$. In this way, we increase the angle of inclination of the SSL. For $\beta_1=\dfrac{\varphi(t_f)}{2}+\pi$, the SSL direction will be opposite to the direction of the axis X.

Carrying out numerical constructions, we increase β_1 with some step $\Delta\beta_1$ from the value $\frac{\varphi(t_f)}{2}$, controlling the passage of the value $\beta_1 = \frac{\varphi(t_f)}{2} + \pi$. When this value is reached, the constructions stop.

Beneath, we assume that at the end of the next increment $\Delta\beta_1$, we get the value β_1 which strictly less than $\frac{\varphi(t_f)}{2} + \pi$. In this case, we control the passage by the point $A_1(\beta_1)$ the situation when the tangent to the corresponding trajectory becomes parallel to SSL at the instant t_f. We denote such value β_1 by $\bar{\beta}_1$. For $\beta_1 \in \left[\frac{\varphi(t_f)}{2}, \bar{\beta}_1\right]$, the value k is less than 1 and it is separated from 1. Therefore, there are no difficulties with the calculation of the elliptic integrals.

4) Increasing β_1 further, we work in a situation where the resulting $k < 1$, but it is close to 1. We find $\bar{\bar{\beta}}_1$ such that $k(\bar{\bar{\beta}}_1) = 1$. On the interval $\beta_1 \in \left[\bar{\beta}_1, \bar{\bar{\beta}}_1\right]$, the calculation of the elliptic integrals (and hence the solution of equation (7.5) with respect to the unknown k) is carried out by special methods.

Geometrically, the motion that is constructed for $\beta_1 \in \left[\frac{\varphi(t_f)}{2}, \bar{\bar{\beta}}_1\right)$ has the following property. If $\beta_1 \in \left[\frac{\varphi(t_f)}{2}, \bar{\beta}_1\right]$, then there is a point on the trajectory where the tangent is parallel to the SSL. For $\beta_1 \in \left(\bar{\beta}_1, \bar{\bar{\beta}}_1\right)$ on the continuation of the trajectory after the instant t_f (respectively, the integral control cost becomes greater than μ) there is a point where the tangent is parallel to the SSL.

5) By increasing β_1 from $\bar{\bar{\beta}}_1$, we get the value $k > 1$. Here we use again special methods to find k. The resulting trajectory, when it continues after the instant t_f, intersects the SSL. We increase β_1 until the point of the intersection of the trajectory with the SSL coincides with the point $A_1(\beta_1)$. We denote the corresponding β_1 by $\widetilde{\beta}_1$. The curve constructed for such β_1 has the symmetric (relatively to the axis X) curve. The union of these two symmetric parts forms the curve A_1.

6) It is verified that if $\beta_1 = \frac{\varphi(t_f)}{2} + \pi$ is implemented at the current step, then the point $A_1\left(\frac{\varphi(t_f)}{2} + \pi\right)$ lowers onto the axis X from above (at $\beta_1 < \frac{\varphi(t_f)}{2} + \pi$, the point was on the left of the axis X). We stop the increasing β_1.

The constructed curve $\beta_1 \to A_1(\beta_1)$, where $\beta_1 \in \left[\frac{\varphi(t_f)}{2}, \frac{\varphi(t_f)}{2} + \pi\right]$, approaches the axis X at the right angle. Taking into account the reflection about the axis X, we obtain the entire curve A_1, and it is a closed smooth curve.

7) Let us analyze the existence and uniqueness of the solution of equation (7.5). It is convenient to consider two cases: $\beta_1 \in \left[\frac{\varphi(t_f)}{2}, \varphi(t_f)\right]$ and $\beta_1 \in \left(\varphi(t_f), \frac{\varphi(t_f)}{2} + \pi\right]$. The second case is not possible for $\varphi(t_f) \geq 2\pi$.

Let $\beta_1 \in \left[\frac{\varphi(t_f)}{2}, \varphi(t_f)\right]$. For $k=0$, the right-hand side of (7.5) is $\varphi^2(t_f) < \varphi^2_{\max} = t_f\mu$. For $k=1$, the following expression is known for an integral of the first kind [12, p. 37, formula (35)]:

$$\int_0^{\varphi} \frac{d\gamma}{\sqrt{1-k^2\sin^2\gamma}} = \ln\tan\left(\frac{\pi}{4}+\frac{\varphi}{2}\right).$$

If $\varphi = \frac{\pi}{2}$, then such an integral is equal to $+\infty$. Hence, taking into account the fact that in the case under consideration the integration interval contains $\frac{\pi}{2}$, it follows that the first bracket in (7.5) is equal to $+\infty$. The second bracket is positive as the integral of a non-negative (not equal to zero identically) function on the integration interval of length $\frac{\varphi(t_f)}{2} > 0$. Thus, the existence of a solution for some $k \in (0,1)$ follows from the fact that the right-hand side of equation (7.5) is less than the left one for $k=0$ and greater it for $k\to 1$. Note that for $k>1$ the integral in the first bracket of the right-hand side of (7.5) is not defined in real numbers because the integration interval contains $\frac{\pi}{2}$. Therefore, there is no solution of (7.5) among such values of k.

Let now $\beta_1 \in \left(\varphi(t_f), \frac{\varphi(t_f)}{2}+\pi\right]$. Here also for $k=0$, the right-hand side of (7.5) is equal to $\varphi^2(t_f)$. The integration interval in the considering case belongs to the interval $\left(-\frac{\pi}{2}, \frac{\pi}{2}\right)$. Since in (7.5) the radicand expressions must be non-negative, then for each value β_1 we can specify the maximum value $k^*(\beta_1) > 1$ such that for all $k \in \left[0, k^*(\beta_1)\right]$ the right-hand side of (7.5) will be defined (and finite). The value $k^*(\beta_1)$ is given by the formula

$$k^*(\beta_1) = 1/\alpha(\beta_1), \quad \alpha(\beta_1) = \max\left\{\left|\sin\left(\frac{-\beta_1+\pi}{2}\right)\right|, \left|\sin\left(\frac{\varphi(t_f)-\beta_1+\pi}{2}\right)\right|\right\}.$$

If the right-hand side of (7.5) for $k = k^*(\beta_1)$ is greater than or equal to $t_f\mu$, then the solution of the equation (7.5) exists on the interval $(0, k^*(\beta_1)]$. Otherwise, there is no solution on this interval. For $k > k^*(\beta_1)$, the right-hand side of (7.5) is not defined, and, therefore, there are no solutions.

The proof of the uniqueness of solutions in the cases under consideration is based on the analysis of the derivative of the right-hand side with respect to the parameter k. One can verify that such a derivative is positive for all admissible values $k>0$ for which the right-hand side of (7.5) is defined (in the first case for $k \in (0,1)$ and in the second case for $k \in (0, k^*(\beta_1))$). This implies the uniqueness of the (7.5) solution with respect to k (in the second case, if it exists).

The value $\widetilde{\beta}_1$ introduced in the item 5) is the largest value at which for all $\beta_1 \in \left[\frac{\varphi(t_f)}{2}, \widetilde{\beta}_1\right]$ the solution of (7.5) exists and is unique.

7.2. **Curve A_3.** If $\widetilde{\beta}_1 < \frac{\varphi(t_f)}{2}+\pi$, then the point $A_1(\widetilde{\beta}_1)$ is to the left of the axis X. The angle between the velocity vector at the point $A_1(\widetilde{\beta}_1)$ and the direction of the corresponding SSL is greater than zero. Let us denote such an angle as $\widetilde{\beta}_3$. We continue the curve A_1 with the curve A_3.

When constructing the curve A_3, we enumerate all controls with one instant of sign change from "+" to "−", giving at the instant t_f the value of the angle equal to $\varphi(t_f)$. Each trajectory is completely determined by the values t_f, μ, $\varphi(t_f)$, and the angle β_3 of the trajectory inclination at the instant of crossing the SSL (the angle is counted counterclockwise from the direction of the velocity vector to the direction of the SSL; in Fig. 4b,c, this angle is indicated by β'). Therefore, we can, taking an auxiliary starting point on the SSL, separately consider the part of the motion from this point *in the direct time* with a negative control that satisfies the PMP and a given angle β_3. We build such a part of the motion until the change of the angle φ on it reaches the fixed meaning $\varphi_3 \geq 0$ by modulo. Then, *in the reverse time*, from the same auxiliary point at the same angle β_3, we consider a motion with positive control on the time interval, on which the change in the angle φ will be $\varphi_3 + \varphi(t_f)$.

The value φ_3 with taken β_3 is chosen so that the total time in these two intervals is equal to t_f and the integral control cost is equal to μ. Pasting two resulting trajectories into one through their common starting point, we obtain a trajectory on the interval $[0, t_f]$, the resulting angle change along which is equal to $\varphi(t_f)$. By transferring its initial point to the origin of the original system x, y and combining the direction of the velocity vector at the initial instant with the direction of the axis x, we obtain the required motion. Let us denote its end point by $A_3(\beta_3)$.

We collect the curve A_3 by increasing the angle $\beta_3 \geq \widetilde{\beta}_3$. We control that the branch of the curve, which is built in the reverse time, does not go to the SSL again. The latter determines the largest angle $\widehat{\beta}_3 \in [\widetilde{\beta}_3, \pi]$ of the inclination of the velocity vector to the SSL at the auxiliary starting point.

The above conditions lead to the following system of the relations:

$$t_f = \int_0^{\varphi_3} \frac{d\varphi}{\sqrt{c_* - 2\rho\cos(\varphi+\beta_3)}} + \int_0^{\varphi_3+\varphi(t_f)} \frac{d\varphi}{\sqrt{c_* - 2\rho\cos(\varphi+\beta_3)}}, \tag{7.6}$$

$$\mu = \int_0^{\varphi_3} \sqrt{c_* - 2\rho\cos(\varphi+\beta_3)}\, d\varphi + \int_0^{\varphi_3+\varphi(t_f)} \sqrt{c_* - 2\rho\cos(\varphi+\beta_3)}\, d\varphi. \tag{7.7}$$

Given that the auxiliary starting point lies on the SSL, we set $c_* = 2\rho\cos\beta_3$. Multiplying equalities (7.6) and (7.7), we get the equation for φ_3. For each β_3 in some range $[\widetilde{\beta}_3, \widehat{\beta}_3]$, we find from such an equation the only φ_3, and then the only ρ from the relation (7.7). Based on the obtained values of φ_3 and ρ, we construct two branches of the desired geometric curve. We transfer the glued curve to the origin of coordinates of the original system, as described above.

The value of $\widehat{\beta}_3 \in (\widetilde{\beta}_3, \pi)$ at which the construction stops is determined by the realization of at least one of the conditions: a) a branch of the curve, which is built in reverse time from an auxiliary starting point, falls on the SSL for the second time; b) the value of φ_3 becomes zero.

The enumeration of the values $\beta_3 \in [\widetilde{\beta}_3, \widehat{\beta}_3]$ gives the curve A_3. The curve A_2 is symmetric to the curve A_3 relatively to the axis X. By virtue of Lemma 4.2, the reverse control is carried out to each point of the curve A_2.

It is possible that with β arbitrarily close to $\widetilde{\beta}_3$ from above, the system (7.6) and (7.7) has no solution. In this case, we set $\widehat{\beta}_3 = \widetilde{\beta}_3$. We consider the curve A_3 to be degenerate and consist of a single point $A_3(\widetilde{\beta}_3)$. Similarly, we consider the curve A_2 to be degenerate.

7.3. **Curve A_6.** Let $\widehat{\varphi}_{6,1} \geq 0$ be the value φ_3 obtained for $\beta_3 = \widehat{\beta}_3$. When constructing the curve A_6, we consider $\widehat{\varphi}_{6,1} > 0$ and take $\varphi_{6,1}$ as a one-dimensional parameter, decreasing it from the value $\widehat{\varphi}_{6,1}$. The motion leading under the considered $\varphi_{6,1}$ to the point $A_6(\varphi_{6,1})$ consists of the three parts equal in angular value respectively to $-\varphi_{6,2}$ (the part lies to the right of the SSL), $\varphi_{6,2} + \varphi_{6,1} + \varphi(t_f)$ (this part lies to the left of the SSL), and $-\varphi_{6,1}$ (to the right of the SSL). Here $\varphi_{6,2}$, $\varphi_{6,1}$, and $\varphi(t_f)$ are assumed to be positive. The following equality holds:

$$2\pi - 2\beta_6 - \varphi_{6,2} - \varphi_{6,1} = \varphi(t_f). \tag{7.8}$$

The angle β_6 is defined in the same way as the angle β_3, but it corresponds to the second hit (in the direct time) of the motion on the SSL.

Let us write the following relations:

$$t_f = \int_0^{\varphi_{6,2}} \frac{d\varphi}{\sqrt{c_* - 2\rho\cos(\varphi+\beta_6)}} + \int_0^{\varphi_{6,1}} \frac{d\varphi}{\sqrt{c_* - 2\rho\cos(\varphi+\beta_6)}} + \int_0^{\varphi_{6,2}+\varphi_{6,1}+\varphi(t_f)} \frac{d\varphi}{\sqrt{c_* - 2\rho\cos(\varphi+\beta_6)}},$$

$$\mu = \int_0^{\varphi_{6,2}} \sqrt{c_* - 2\rho\cos(\varphi+\beta_6)}\, d\varphi + \int_0^{\varphi_{6,1}} \sqrt{c_* - 2\rho\cos(\varphi+\beta_6)}\, d\varphi + \int_0^{\varphi_{6,2}+\varphi_{6,1}+\varphi(t_f)} \sqrt{c_* - 2\rho\cos(\varphi+\beta_6)}\, d\varphi.$$

We set $c_* = 2\rho\cos\beta_6$ in them. The given above relations together with equality (7.8) give a system with respect to β_6 and ρ for a fixed $\varphi_{6,1}$.

We construct the curve A_6 until it hits the axis X with the equality $\varphi_{6,1} = \varphi_{6,2}$. By Lemma 4.2, considering a curve symmetric relatively to the axis X, we obtain the combined curve A_6. The curve A_6 connects the ends of the curves A_3 and A_2. It is smoothly conjugated with the curves A_3 and A_2. The curve A_6 is not plotted if $\widehat{\varphi}_{6,1} = 0$.

7.4. **The φ-section boundary without the curve A_6.** The value of $\widehat{\varphi}_{6,1}$ depends on $\varphi(t_f)$. We verified numerically that there is some $\varphi^*(t_f)$ such that $\widehat{\varphi}_{6,1} = 0$ for $\varphi(t_f) = \varphi^*(t_f)$ and $\widehat{\varphi}_{6,1} > 0$ if $\varphi(t_f) < \varphi^*(t_f)$. In the case $\varphi(t_f) > \varphi^*(t_f)$ there are no extremal controls with two instants of sign change, i.e. belonging to type U_6. Therefore, for $\varphi(t_f) > \varphi^*(t_f)$, the curve A_6 is not constructed. We can say that it degenerates to a point for $\varphi(t_f) = \varphi^*(t_f)$. Such a point lies on the auxiliary axis X. It is also the last point $A_3(\widehat{\beta}_3)$ of the curve A_3. The switching straight line corresponding to $\widehat{\beta}_3$ runs along the axis X, but it has opposite direction.

When $\varphi(t_f)$ becomes greater than $\varphi^*(t_f)$, then for the last point $A_3(\widehat{\beta}_3)$ of the curve A_3, as with $\varphi(t_f) = \varphi^*(t_f)$, the condition $\varphi_3 = 0$ is fulfilled. In this case, the point $A_3(\widehat{\beta}_3)$ is again located to the left of the axis X. In system (7.6), (7.7), the first integral terms on the right side are become equal to zero. It can be shown that this system transforms into system (7.1), (7.2). The corresponding proof involves replacing the variable φ in the integrand with a new variable

$\varphi^\flat = \varphi(t_f) - \varphi$. Additionally, we take into account that $\beta_3 = \beta_1 - \varphi(t_f)$, and also that the relation $c_* = 2\rho\cos\beta_3$ in (7.6), (7.7) due to (5.7) coincides with the expression for c_* in (7.1), (7.2).

For $\varphi(t_f) > \varphi^*(t_f)$ after constructing the curve A_3 we construct the second piece of the curve A_1, increasing β_1, but now starting from $\beta_1 = \widehat{\beta}_3 + \varphi(t_f)$, until the curve hits the axis X. As $\varphi(t_f)$ increases, the arc A_3 "shrinks", then it is degenerated into a point and disappears. Before the curve A_3 (and, accordingly, A_2) degenerates, the boundary of the φ-section consists of the curves A_3, A_2 and two pieces of the curve A_1. After the curve A_3 degenerates, the boundary of the set $G_\varphi(t_f,\mu)$ consists only of the curve A_1.

8. Results of numerical construction of the three-dimensional reachable set and its φ-sections

We reduce the study of a three-dimensional reachable set to the study of its φ-sections with $\varphi \geq 0$. For $\varphi < 0$, φ-sections $G_\varphi(t_f,\mu)$ can be obtained from the φ-sections for $\varphi > 0$ due to the symmetry property described in Section 4.4.

1) Let us start with the case when the values t_f and μ are such that the maximum possible $\varphi_{\max} = \sqrt{t_f\,\mu} \leq 2\pi$. In this case, for each φ-segment $G_\varphi(t_f,\mu)$, where $0 < \varphi < \varphi_{\max}$, its boundary consists of successively connected curves A_1, A_3, A_6 and A_2. That is, the curve $\mathcal{A} = A_1 \cup A_3 \cup A_6 \cup A_2$ has no self-intersections and forms the boundary of the set $G_\varphi(t_f,\mu)$. For $\varphi(t_f)$ close to $\varphi_{\max}$, the curves A_6, A_3, A_2 degenerate and the boundary of the φ-section is determined only by the curve A1. If $\varphi = 0$, then the curve A_1 degenerates. The boundary of the set $G_\varphi(t_f,\mu)$ is composed of the curves A_3, A_6, A_2. We close the curves A_3 and A_2 at a singular point corresponding to the control $u \equiv 0$. Note that for $\varphi = 0$, according to Theorem 6.3, the set of points generated by the control type U_5 (curve A_5) coincides with the curve A_6.

In Fig. 6 for $\mu = 4$, $t_f = 4$, there is a visual representation of the set $G(t_f,\mu)$ as a set of its φ-sections derived with some step $\triangle\varphi$. The surfaces that form the boundary of the three-dimensional reachable set are constructed on the basis of these φ-sections using triangulation. We keep the designations A_1, A_3, A_6, and A_2 for such surfaces.

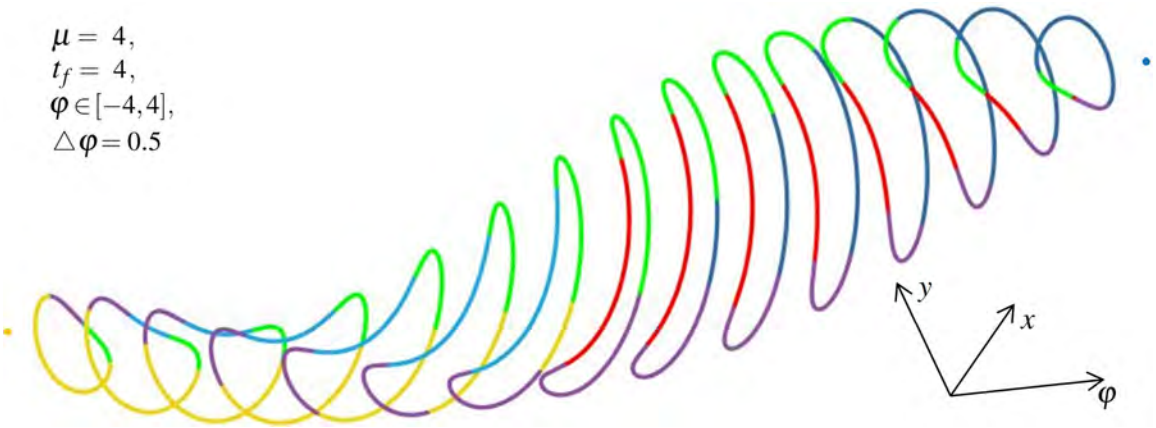

FIGURE 6. A collection of φ-sections for a three-dimensional reachable set

Figure 7 shows the φ-section for $\mu = 4$, $t_f = 4$, $\varphi(t_f) = 2$. The examples of motions leading to the curves A_1, A_3, A_6 are presented. The SSL corresponding to these motions are also shown. The SSL for the motion leading to a point on the curve A_1 visually touches the trajectory of this motion. In fact, the trajectory lies on one side of the SSL (namely, on the left). The boundary of the φ-section is formed by sequentially connecting the curves A_1, A_3, A_6, and A_2. Such a case is the simplest on application of Theorem 6.3 to analyze the boundary of a φ-section.

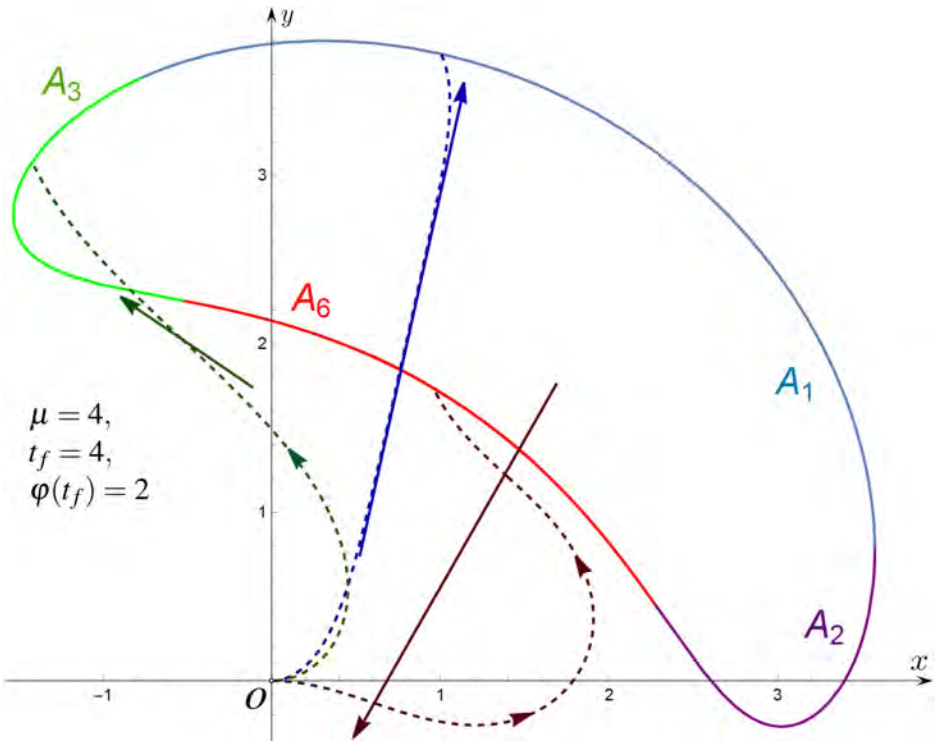

FIGURE 7. The boundary of the φ-section is completely determined by the connection of the curves A_1, A_2, A_3, and A_6

As the value $\varphi = \varphi(t_f)$ increases, the curve A_6 "shrinks", and at some φ it disappears. The φ-section becomes convex. The convexity property is preserved as $\varphi(t_f)$ grows further.

For some small range of values $\varphi(t_f)$ after the curve A_6 disappears, the boundary of the φ-section is determined by the curves A_1, A_3 and A_2. In this case, the curve A_1 has two pieces. The second piece that appears additionally connects the curves A_3 and A_2 instead of the disappeared curve A_6. The corresponding example is shown in Fig. 8.

With a further increase of $\varphi(t_f)$, the curves A_3 and A_2 disappear. The boundary of the φ-section is completely determined by the curve A_1 (see Fig. 9). This curve is symmetric relatively to the axis X.

Figs. 8 and 9 are calculated for $\mu = 4$, $t_f = 4$. The value $\varphi(t_f)$ is equal to 3.6 and 3.8 respectively. In these figures, the parts of the curve A_1, which were mentioned in Section 7.1 (items 3), 4), 5)), are highlighted in different colors. The part 1 corresponds to the item 3) in Section 7.1, the part 2 (two segments) is described in the item 4), and the part 3 is described in the item 5). The variants of the motions leading to these parts, as well as the corresponding SSL, are also shown.

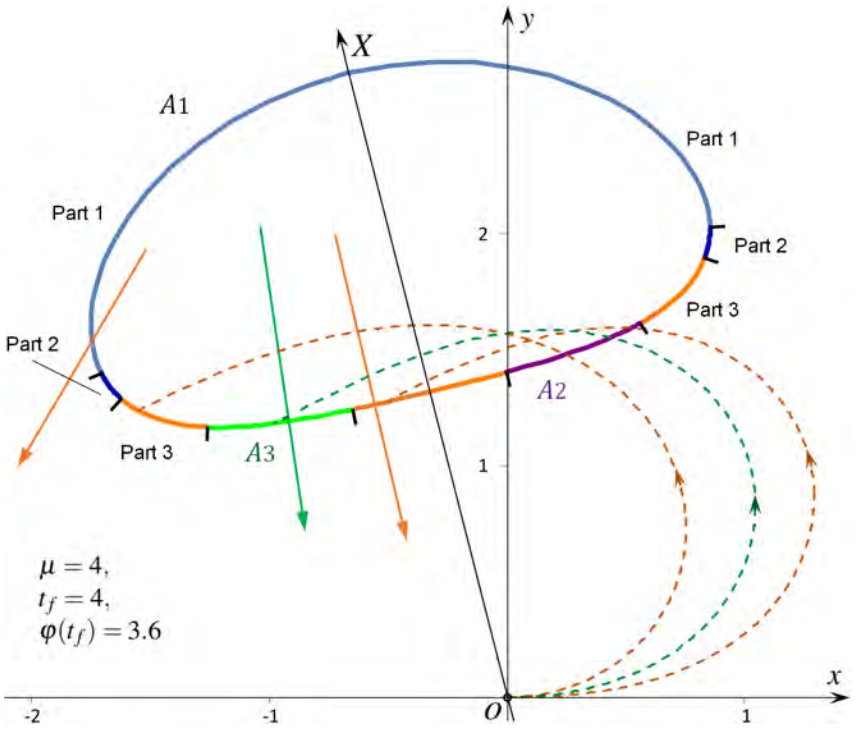

FIGURE 8. The boundary of the φ-section is determined by the curves A_1, A_3, and A_2

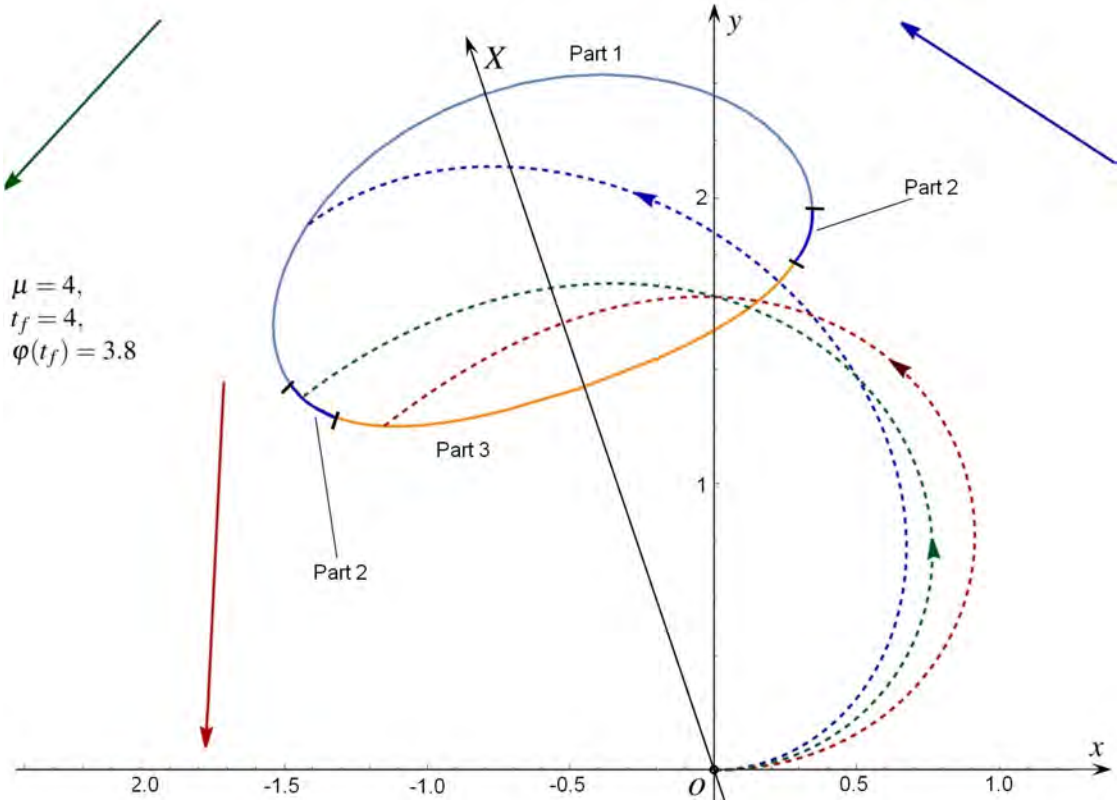

FIGURE 9. The boundary of the φ-section is determined only by the curve A_1

Figure 10 shows the three-dimensional set $G(t_f,\mu)$ for $t_f=(1.5\pi)^2$ and $\mu=1$ from two points of view. The parts of the boundary to which various types of controls lead are highlighted in color: U_1 is a positive control (blue), U_4 is a negative control (yellow), U_3 is a control with one instant of sign change from "+" to "−" (green), and U_2 is a control with one instant of sign change from "−" to "+" (purple). The point $z^0(t_f)$, for which the control is identically equal to zero, lies at the junction of the four indicated parts. The black lines mark the contours of the cross-sections of the three-dimensional set $G(t_f,\mu)$ with some step along the axis φ. This picture can be compared with a similar Fig. 2 which was made for the geometric constraint. The picture is different from Fig. 2 boundary by smoothness for extreme values φ, as well as a smooth joint of the surfaces A_6 and A_5 (which consist, respectively, of the curves A_6 and A_5) with the surfaces A_2 and A_3 (they consist of the curves A_2 and A_3). The non-smoothness of joining the surfaces A_6 and A_5 at $\varphi=0$ is preserved.

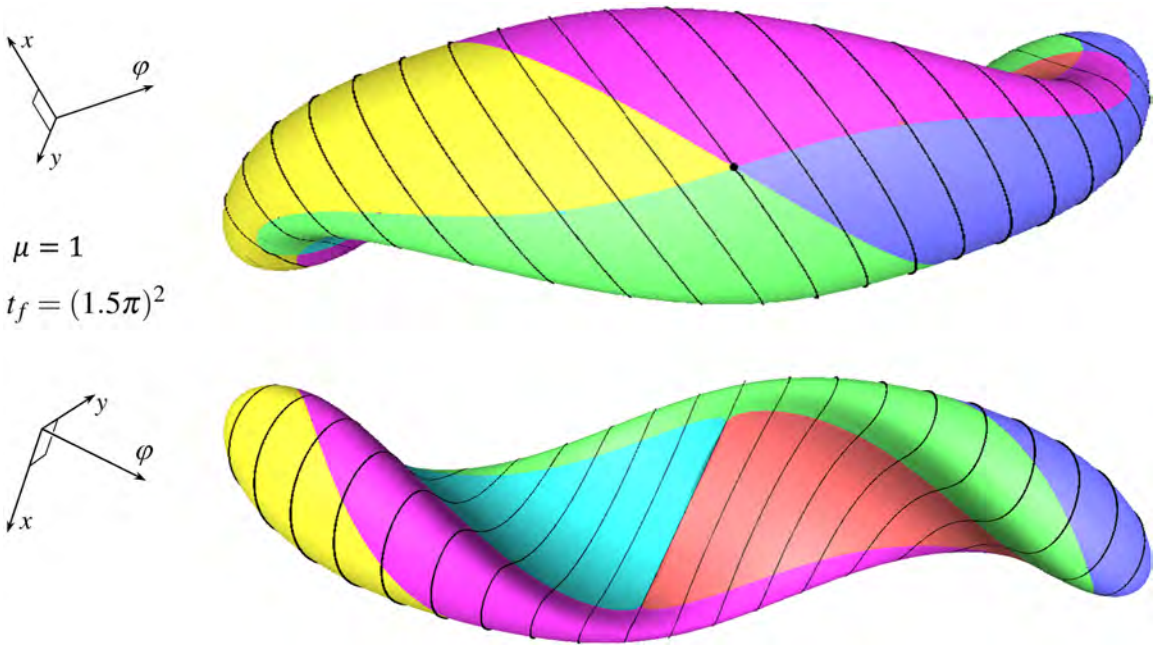

FIGURE 10. Three-dimensional reachable set from two points of view

2) The three-dimensional reachable set $G(t_f,\mu)$ calculated at $\mu=100$ for the instant $t_f=0.95$ is shown on the left of Fig. 11 (here we are already dealing with the case $\varphi_{\max}>2\pi$). The set $G(t_f,\mu)$ is not simply connected: there is a cavity that does not belong to it. It is not visible when we look at the set from the outside.

To show that the three-dimensional set is not simply connected, Fig. 11 on the right shows its φ-section $G_\varphi(t_f,\mu)$ for $\varphi=0$. Since $\varphi=0$, then the auxiliary axis X, relatively to which the φ-section is symmetric, coincides with the axis x. There is no curve A_1 on $\partial G_\varphi(t_f)$. The point $\left(x^0(t_f),y^0(t_f)\right)^{\mathsf{T}}$ belongs to the given φ-section and is located on the axis x. Curves A_3 and A_2 are symmetric to each other and depart from this point. Their arcs up to the point P_1 of the first intersection give the "outer" boundary of the φ-section. The open arcs A_3 and A_2 from the point P_1 to the point P_2 of the second intersection lie in the interior of the φ-section. The curve A_6 and adjacent parts of the curves A_3 and A_2 after the point P_2 form the boundary of the "hole" that does not belong to $G_\varphi(t_f,\mu)$. The dashed lines show the trajectories of four motions, leading

onto the boundary of the φ-section (and, therefore, to the boundary of the three-dimensional reachable set). The trajectories leading to the points e_1, e_2 and e_3 have one inflection point (the control sign change point). The trajectory leading to the point e_4 on the curve A_6 has two inflection points (two points of control sign change).

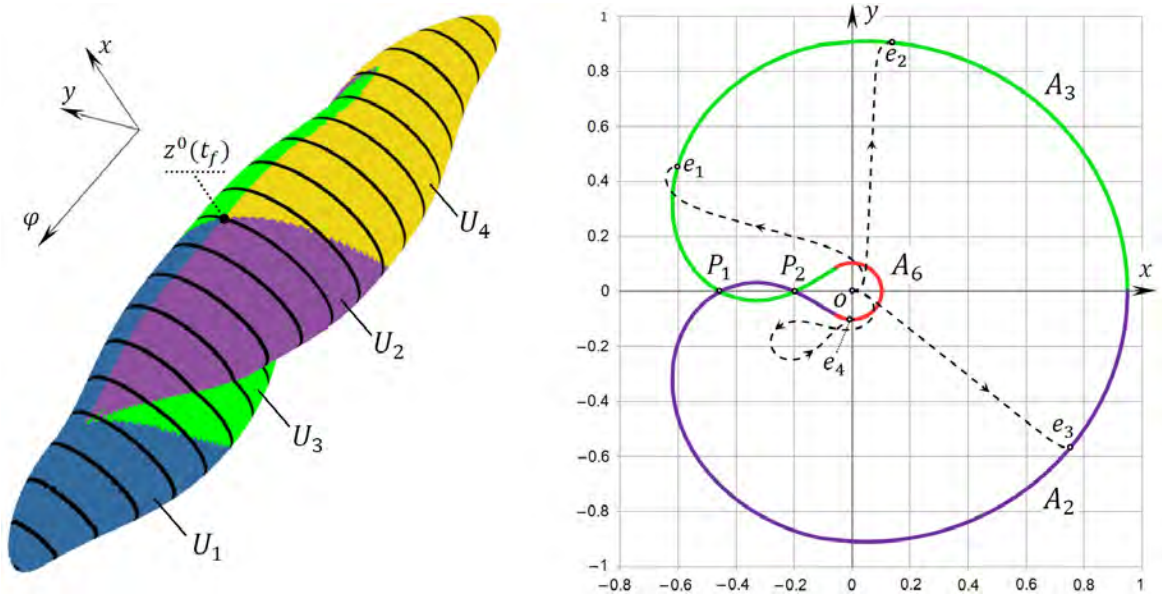

FIGURE 11. Three-dimensional reachable set $G(t_f,\mu)$ (left) and its φ-section for $\varphi = 0$ (right); $\mu = 100$, $t_f = 0.95$

Further evolution of the φ-sections $G_\varphi(t_f,\mu)$ is shown in Fig. 12. For each $\varphi(t_f)$, three motions leading to the curves A_1, A_3, and A_6 are shown. The corresponding SSLs are also shown.

The non-connectivity of the φ-section stays for $\varphi(t_f) = 0.5$ (Fig. 12a). The outer boundary of the φ-section is then determined by the curve A_1 and the arcs of the curves A_3 and A_2 up to the point P_1 of their first intersection. The curve A_6 and the parts of the curves A_3 and A_2 adjacent to it up to the point P_2 form the boundary of the "hole". In Figs. 12b and 12c, the φ-sections are simply connected. The boundary of the φ-sections is determined by the curve A_1 and the arcs of the curves A_3 and A_2 adjacent to it up to the point P_1 of their first intersection.

The example in Fig. 13 is selected for $t_f \approx 1.1244$, $\mu = 100$, $\varphi(t_f) = 0$ so that to show the motions in the form of lemniscates. Here the curve A_6 has degenerated into the point, which coincides with the origin. The figure on the right shows six curves of the lemniscate family. All trajectories of the family represent the same geometric lemniscate, but the point of its attachment to the origin of the original system changes. Each trajectory starts and ends at the origin with the direction of the velocity vector along the axis x. With an arbitrarily small decrease of μ, a "hole" appears and the origin point no longer belongs to the φ-section at $\varphi = 0$.

A detailed study of the closed trajectories of motion (closed Euler elasticae) is contained in paper [11]. It is proven that the lemniscate is not globally optimal in the problem of minimizing functional (1.2) when identifying the angle modulo 2π. This motion is locally optimal.

In Fig. 14 approximately in the same perspective as for Fig. 1, the three-dimensional reachable sets $G(t_f,\mu)$ for $\mu = 1$ and $t_f = \pi^2, (2\pi)^2, (3\pi)^2, (4\pi)^2$ are shown. We can compare them to the reachable sets under the geometric constraint.

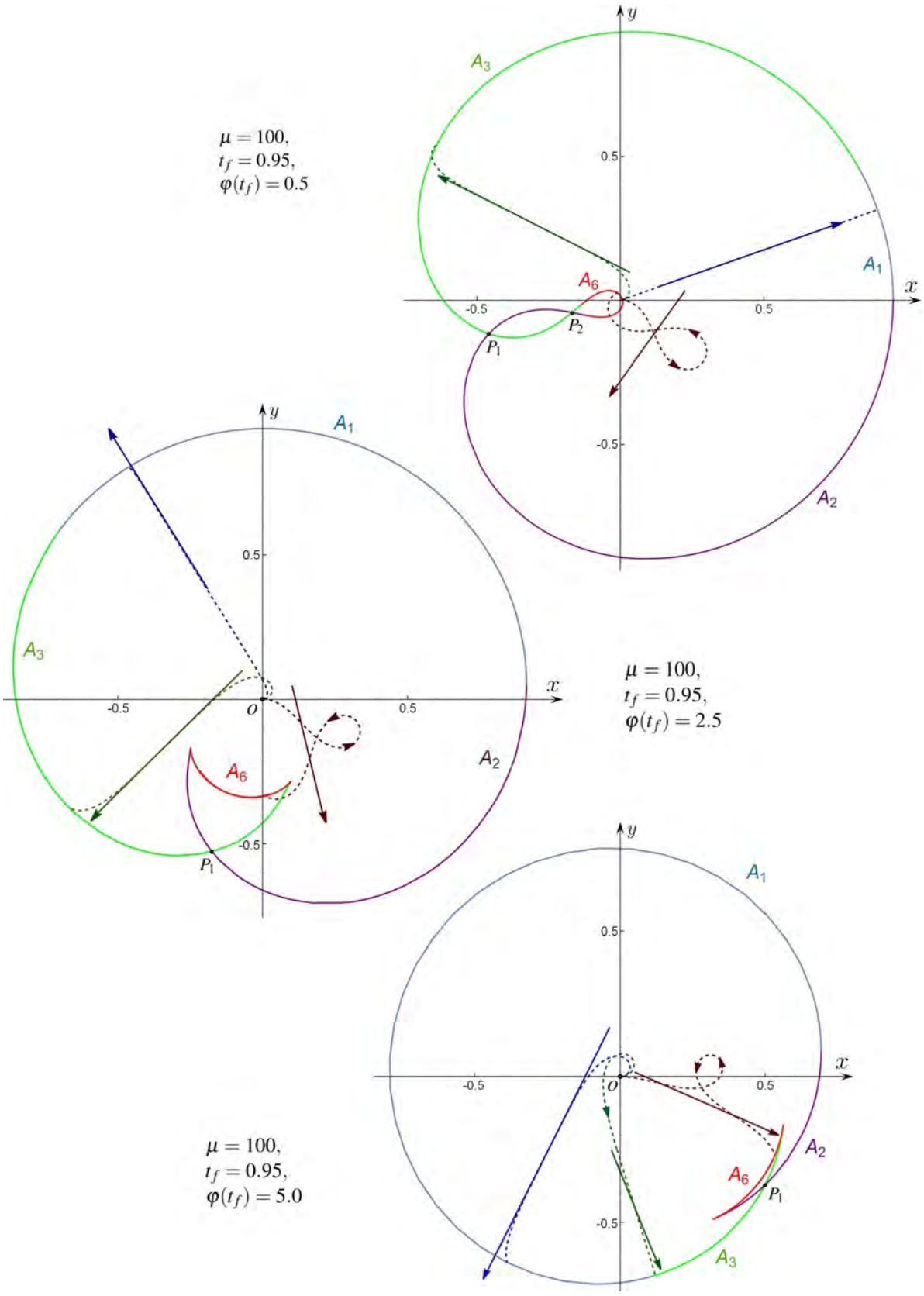

FIGURE 12. Evolution of φ-sections with growth of $\varphi(t_f)$

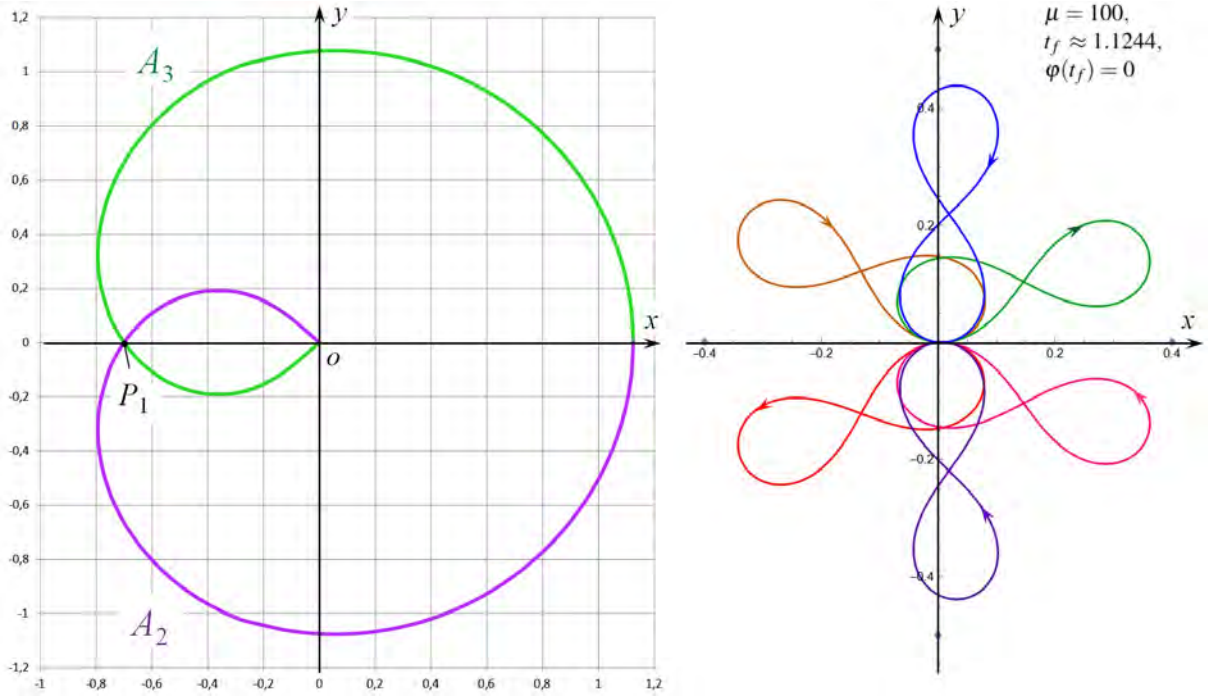

FIGURE 13. An example of motion trajectories (Euler elasticae) in the form of lemniscates

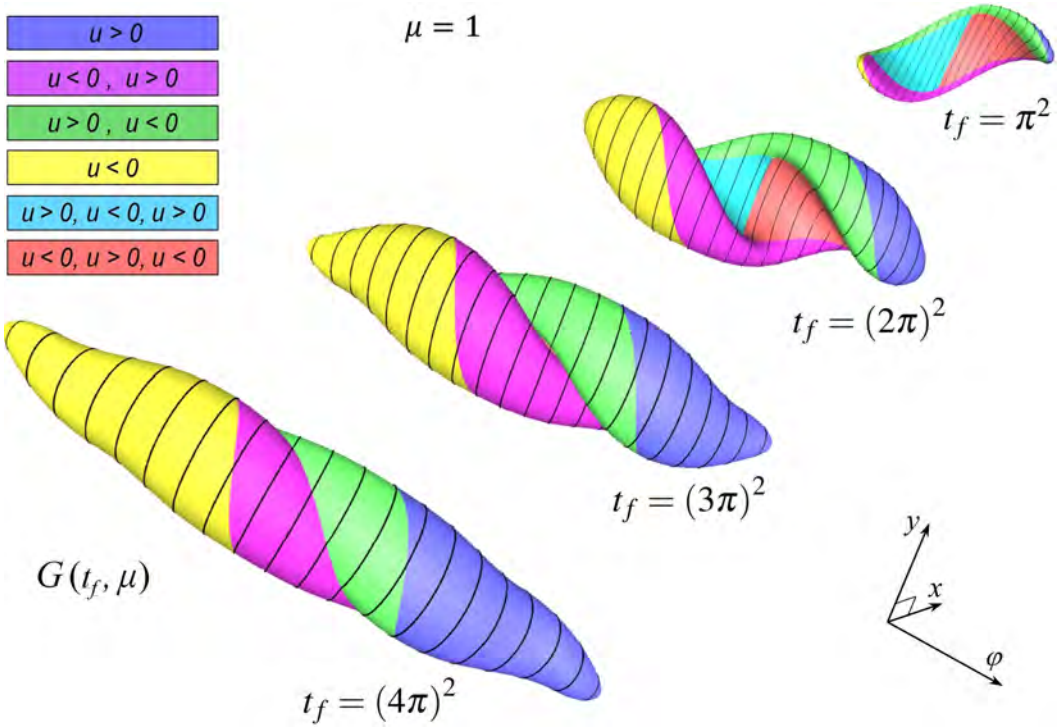

FIGURE 14. Evolution in time of a three-dimensional reachable set $G(t_f, \mu)$ under the integral quadratic constraint

9. Identification of angles modulo 2π

In applied problems, the angle φ is often identified by modulo 2π. Using the algorithm for constructing the set $G(t_f,\mu)$, it is easy to construct the reachable set $\breve{G}(t_f,\mu)$ by equating angles differing by a shift $k2\pi$. The following formula is valid:

$$\breve{G}_{\breve{\varphi}}(t_f,\mu)=\bigcup G_{\varphi}(t_f,\mu),\quad \varphi=\breve{\varphi}\pm k2\pi,\ \ k=0,1,2...,\quad \breve{\varphi}\in[-\pi,\pi).$$

This formula itself says that the set $\breve{G}(t_f,\mu)$ looks geometrically "very complex". In Fig. 15, the sets $\breve{G}(t_f,\mu)$ are shown for $\mu=1$, $t_f=(1.5\pi)^2$ and $t_f=(2\pi)^2$.

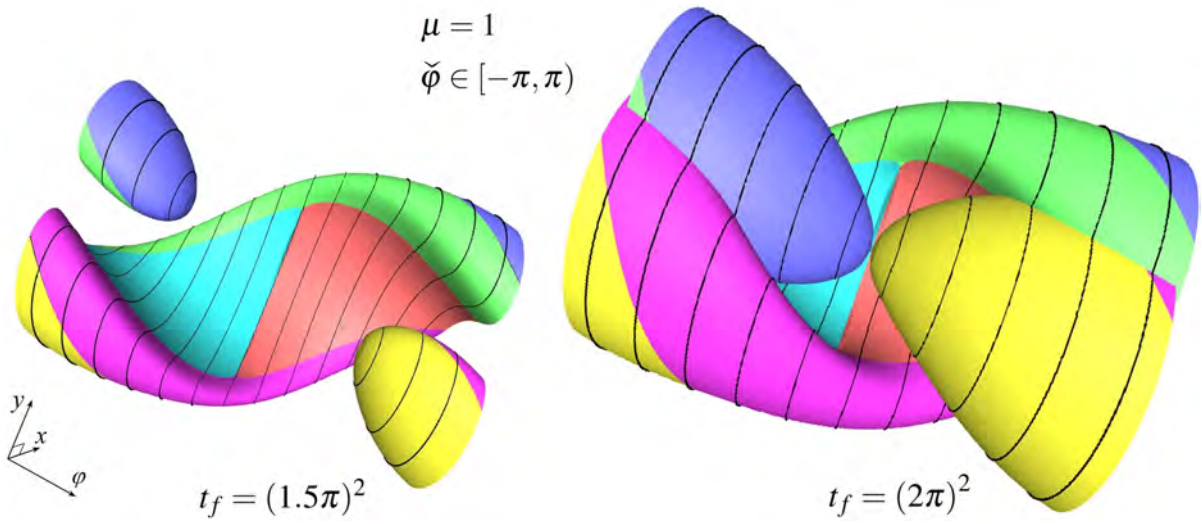

FIGURE 15. Three-dimensional reachable set $\breve{G}(t_f,\mu)$ for the case when the angles φ are identified by modulo 2π

10. Finding globally optimal Euler elasticae

We assume that a point $(\breve{x},\breve{y})^{\mathsf{T}}$ and an angle $\breve{\varphi}\in(-\pi,\pi]$ are fixed for the instant t_f. Let us denote by the symbol μ^* the minimal value of the integral functional (1.2), under which the transition of system (2.1) is possible to the point $(\breve{x},\breve{y})^{\mathsf{T}}$ at the time t_f with the angle $\breve{\varphi}$ identified by modulo 2π. It is required to specify a method for calculating the optimal value μ^*, as well as to construct all the motions (globally optimal Euler elasticae), each of which goes from the initial state to the final one with the optimal index μ^*. For brevity, we write $\breve{a}=(\breve{x},\breve{y})^{\mathsf{T}}$.

10.1. **Global minimum and optimal elasticae: φ-sections for their search.** We exclude the point $\breve{x}=t_f$, $\breve{y}=0$ with $\breve{\varphi}=0$, because the transition to the point is carried out by $u(t)\equiv 0$ and, therefore, $\mu^*=0$ is the minimal value of the integral functional. For other points, the transfer at the time t_f is possible only when $\sqrt{\breve{x}^2+\breve{y}^2}<t_f$.

Let

$$\mu_0=\min\{\mu:\breve{a}\in G_{\breve{\varphi}}(t_f,\mu)\},$$

$$\mu_-=\min\{\mu:\breve{a}\in G_{\breve{\varphi}-2\pi}(t_f,\mu)\},\qquad \mu_+=\min\{\mu:\breve{a}\in G_{\breve{\varphi}+2\pi}(t_f,\mu)\}.$$

1) Firstly, let us assume that $\breve{\varphi} \in (0, \pi]$. We will show that to construct all the globally optimal elasticae, one should use only two φ-sections $G_{\breve{\varphi}}(t_f, \mu_0)$ and $G_{\breve{\varphi}-2\pi}(t_f, \mu_-)$. The proof is by contradiction.

Suppose, there exists an integer $k_+ \geq 1$ such that $\breve{a} \in G_{\breve{\varphi}+2\pi k_+}(t_f, \mu^*)$. Taking into account the range $\left[-\sqrt{t_f\mu^*}, \sqrt{t_f\mu^*}\right]$ of the set $G(t_f, \mu^*)$ along the angle coordinate φ, we conclude that $\breve{\varphi} + 2\pi k_+ \leq \sqrt{t_f\mu^*}$.

Since $\breve{\varphi} + 2\pi k_+ > 2\pi$ and the globally optimal motion (the globally optimal Euler elastica) satisfies the PMP, then any control $u(\cdot)$ leading to the point $\breve{a}$ cannot have instants when control sign changes. This follows from Proposition 5.1c. Hence $\breve{a} \in A_1$. At that, the curve A_1 forms the boundary of the φ-section $G_{\breve{\varphi}+2\pi k_+}(t_f, \mu^*)$.

We single out two instants t_1 and t_2 on the considered optimal motion such that $t_2 > t_1$ and $\varphi(t_2) - \varphi(t_1) = 2\pi$. Let us form an auxiliary motion $(\widetilde{x}(\cdot), \widetilde{y}(\cdot))^\mathsf{T}$ on $[t_1, t_2]$ almost similar to the motion appearing in the proof of Lemma 6.1. The only difference is that in the proof of Lemma 6.1 we considered two instants $\bar{t}$ and $\widehat{t}$ such that $\varphi(\widehat{t}\,) = \varphi(\bar{t}\,)$, and here these two instants t_1 and t_2 are such that $\varphi(t_2) = \varphi(t_1) + 2\pi$. Since the symmetry axis X is the same (up to the direction) for the angles φ shifted by 2π, this difference is insignificant.

Figure 16 explains the construction of the auxiliary motion (shown by the red dotted line) on $[t_1, t_2]$. The resulting new motion coincides with the original one on the intervals $[0, t_1]$ and $[t_2, t_f]$. It copies the auxiliary motion on $[t_1, t_2]$. The new motion also arrives to the point $\breve{a}$, but has the value $\varphi(t_f) = \breve{\varphi} + 2\pi k_+ - 4\pi$. Hence, the point $\breve{a}$ belongs to the φ-section $G_{\breve{\varphi}+2\pi k_+ - 4\pi}(t_f, \mu^*)$. However, the PMP is not fulfilled for the constructed motion since the control is discontinuous at the instants t_1 and t_2. Therefore, we have $\breve{a} \in \mathrm{int} G_{\breve{\varphi}+2\pi k_+ - 4\pi}(t_f, \mu^*)$.

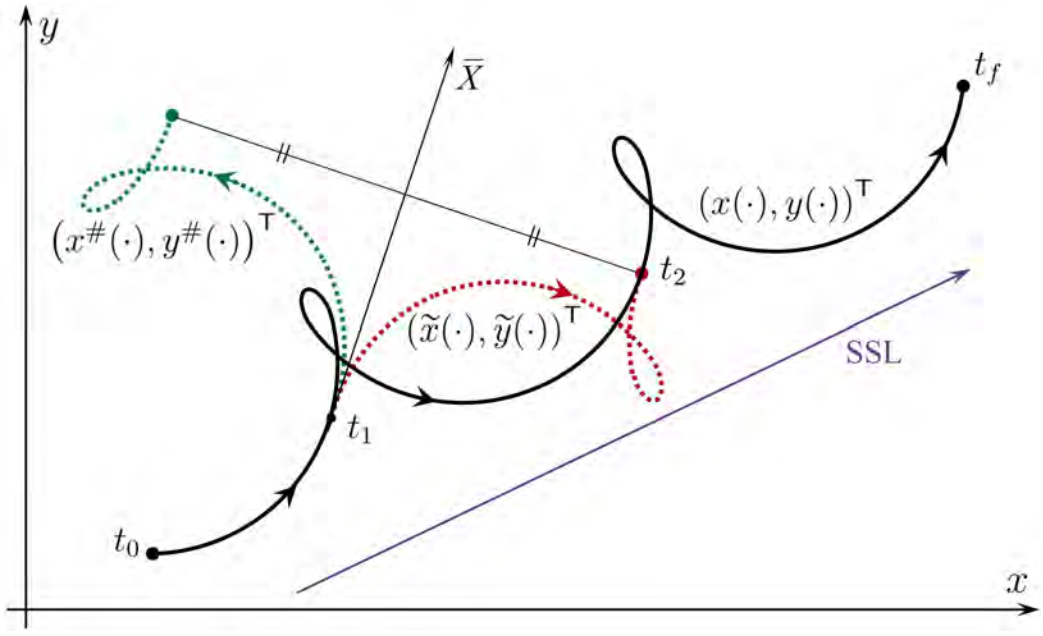

FIGURE 16. Construction of an auxiliary motion in the proof of Theorem 10.1

Let $\breve{z} = (\breve{x}, \breve{y}, \breve{\varphi} + 2\pi k_+ - 4\pi)^\mathsf{T}$. The point $\breve{z}$ cannot coincide with any of the two extreme along coordinate φ points of the three-dimensional "hole" in the set $G(t_f, \mu^*)$. Indeed, if coincident, such a point would lie on the boundary of the set $G(t_f, \mu^*)$ and the PMP would have to

be performed for any motion leading to this point. Since $\breve{\varphi} > 0$, we have $\breve{\varphi} + 2\pi k_+ - 4\pi \neq 0$. Consequently, the point $\breve{z}$ cannot also coincide with the point $(0,0,0)^\mathsf{T}$ of degeneration of the three-dimensional "hole".

As a result, we conclude that it is possible to reduce the value μ to some $\widehat{\mu} < \mu^*$ in such a way that $\breve{a} \in G_{\breve{\varphi}+2\pi k_+ - 4\pi}(t_f, \widehat{\mu})$. This contradicts the fact that μ^* is the minimal value of the integral index for transferring to the point $\breve{a}$ with the angle $\breve{\varphi}$ identified by modulo 2π.

Thus the supposition $\breve{a} \in G_{\breve{\varphi}+2\pi k_+}(t_f, \mu^*)$ is wrong.

The case when there exists a negative integer $k_- \leq -2$ such that $\breve{a} \in G_{\breve{\varphi}+2\pi k_-}(t_f, \mu^*)$ is considered similarly. Here $\breve{\varphi} + 2\pi k_- \leq \breve{\varphi} - 4\pi \leq -3\pi$. Selecting the instants t_1, t_2 such that $t_2 > t_1$ and $\varphi(t_2) - \varphi(t_1) = -2\pi$, we go to a new motion having $\varphi(t_f) = \breve{\varphi} + 2\pi k_- + 4\pi$. And the reasoning is repeated.

Thus, for $\breve{\varphi} \in (0, \pi]$, we obtain $\mu^* = \min\{\mu_0, \mu_-\}$.

2) Let $\breve{\varphi} \in (-\pi, 0)$. Since φ-sections are symmetric for positive and negative φ, in order to find globally optimal elastica, we can restrict ourselves by considering the two φ-sections $G_{\breve{\varphi}}(t_f, \mu_0)$ and $G_{\breve{\varphi}+2\pi}(t_f, \mu_+)$. Therefore, $\mu^* = \min\{\mu_0, \mu_+\}$.

3) If $\breve{\varphi} = 0$, then we should consider three φ-sections $G_{\breve{\varphi}=0}(t_f, \mu_0)$, $G_{\breve{\varphi}=2\pi}(t_f, \mu_+)$, and $G_{\breve{\varphi}=-2\pi}(t_f, \mu_-)$. In this case, $\mu^* = \min\{\mu_0, \mu_+, \mu_-\}$. However, for $\varphi = \pm 2\pi$, the auxiliary axis X is the same and it coincides, up to the direction, with the axis x. Taking into account the symmetry properties from Sections 4.3 and 4.4, we obtain the equality $G_{\varphi=2\pi}(t_f, \mu) = G_{\varphi=-2\pi}(t_f, \mu)$ for any t_f and μ such that $\sqrt{t_f \mu} \geq 2\pi$. Hence, we have $\mu_+ = \mu_-$. Therefore, if $\breve{\varphi} = 0$, then $\mu^* = \min\{\mu_0, \mu_-\} = \min\{\mu_0, \mu_+\}$.

Let us assume that the optimal value μ^* coincides with $\mu_- = \mu_+$. Then $\breve{a} \in \partial G_{\varphi=-2\pi}(t_f, \mu_-)$. Due to the symmetry relative to the axis x, we have $\breve{b} = (\breve{x}, -\breve{y})^\mathsf{T} \in G_{\varphi=-2\pi}(t_f, \mu_-)$. Let $u_{\breve{b}}(t)$, $t \in [0, t_f]$, be a negative control leading to the point $\breve{b}$. Then the positive control $-u_{\breve{b}}(t)$, $t \in [0, t_f]$, leads to the point $\breve{a}$. Therefore, two controls $u_{\breve{a}}(t)$ and $-u_{\breve{b}}(t)$, $t \in [0, t_f]$, lead to the point $\breve{a}$. The first is negative, the second is positive. Both are globally optimal.

The above reasoning gives the following theorem.

Theorem 10.1. *Let a point $\breve{a} = (\breve{x}, \breve{y})^\mathsf{T} \neq (t_f, 0)^\mathsf{T}$ and an angle $\breve{\varphi} \in (-\pi, \pi]$ be given for the instant t_f. Then the globally optimal value μ^* is determined by the formula*

$$\mu^* = \begin{cases} \min\{\mu_0, \mu_-\} & \text{if } \breve{\varphi} \in (0, \pi], \\ \min\{\mu_0, \mu_+\} & \text{if } \breve{\varphi} \in (-\pi, 0), \\ \min\{\mu_0, \mu_-\} = \min\{\mu_0, \mu_+\} & \text{if } \breve{\varphi} = 0. \end{cases}$$

Accordingly, to find all globally optimal elasticae for $\breve{\varphi} \in (0, \pi]$, it is enough to consider two φ-sections $G_{\breve{\varphi}}(t_f, \mu_0)$ and $G_{\breve{\varphi}-2\pi}(t_f, \mu_-)$; for $\breve{\varphi} \in (-\pi, 0)$, we use two φ-sections $G_{\breve{\varphi}}(t_f, \mu_0)$ and $G_{\breve{\varphi}+2\pi}(t_f, \mu_+)$; for $\breve{\varphi} = 0$, it is sufficient to consider two φ-sections $G_{\breve{\varphi}=0}(t_f, \mu_0)$ and $G_{\breve{\varphi}=-2\pi}(t_f, \mu_-)$ (or, what is equivalent, $G_{\breve{\varphi}=0}(t_f, \mu_0)$ and $G_{\breve{\varphi}=2\pi}(t_f, \mu_+)$).

10.2. **An example of four globally optimal elasticae.** Without presenting in this paper a detailed study related to the number of optimal elasticae and their realization on various types of control, we confine ourselves to an example in which four globally optimal elasticae lead to a given point $\breve{a}$ with $\breve{\varphi} = 0$. This example is borrowed from [2]. We will show (see Fig. 17) how it arises when considering the φ-sections mentioned above.

Let us put $t_f = 1$. Fix μ such that $\sqrt{t_f \mu} = \sqrt{\mu} > 2\pi$. The boundary of the φ-section $G_{\varphi=0}(t_f, \mu)$ coincides with the curve $\mathcal{A}$ composed of the sequential connection of the curves A_1, A_3, A_6, and A_2. We are numerically convinced that the part of the curve A_6 located in the half-plane $x \geq 0$ is semi-circumference with the center at the origin. Next, we consider the φ-sections $G_{\varphi=-2\pi}(t_f, \mu)$ and $G_{\varphi=2\pi}(t_f, \mu)$. They match. We verify numerically that the boundary of each of them is a circumference with its center at the origin. We choose $\overline{\mu}$ in such a way that the circumference contains the semi-circumference O_+ of the curve A_6 on the set $G_{\varphi=0}(t_f, \overline{\mu})$ boundary. For any $\mu < \overline{\mu}$, the semi-circumference O_+ lies outside the sets $G_{\varphi=0}(t_f, \mu)$ and $G_{\varphi=-2\pi}(t_f, \mu) = G_{\varphi=2\pi}(t_f, \mu)$. Therefore, for any point $\breve{a} \in O_+$, the global optimal value μ^* coincides with $\overline{\mu}$. Numerical selection of the value $\overline{\mu}$ gives $\mu^* = \overline{\mu} \approx 55$.

The sets $G_{\varphi=0}(t_f, \overline{\mu})$ and $G_{\varphi=-2\pi}(t_f, \overline{\mu}) = G_{\varphi=2\pi}(t_f, \overline{\mu})$ are shown in Fig. 17. For some point $\breve{a}$, the global optimal elasticae are given.

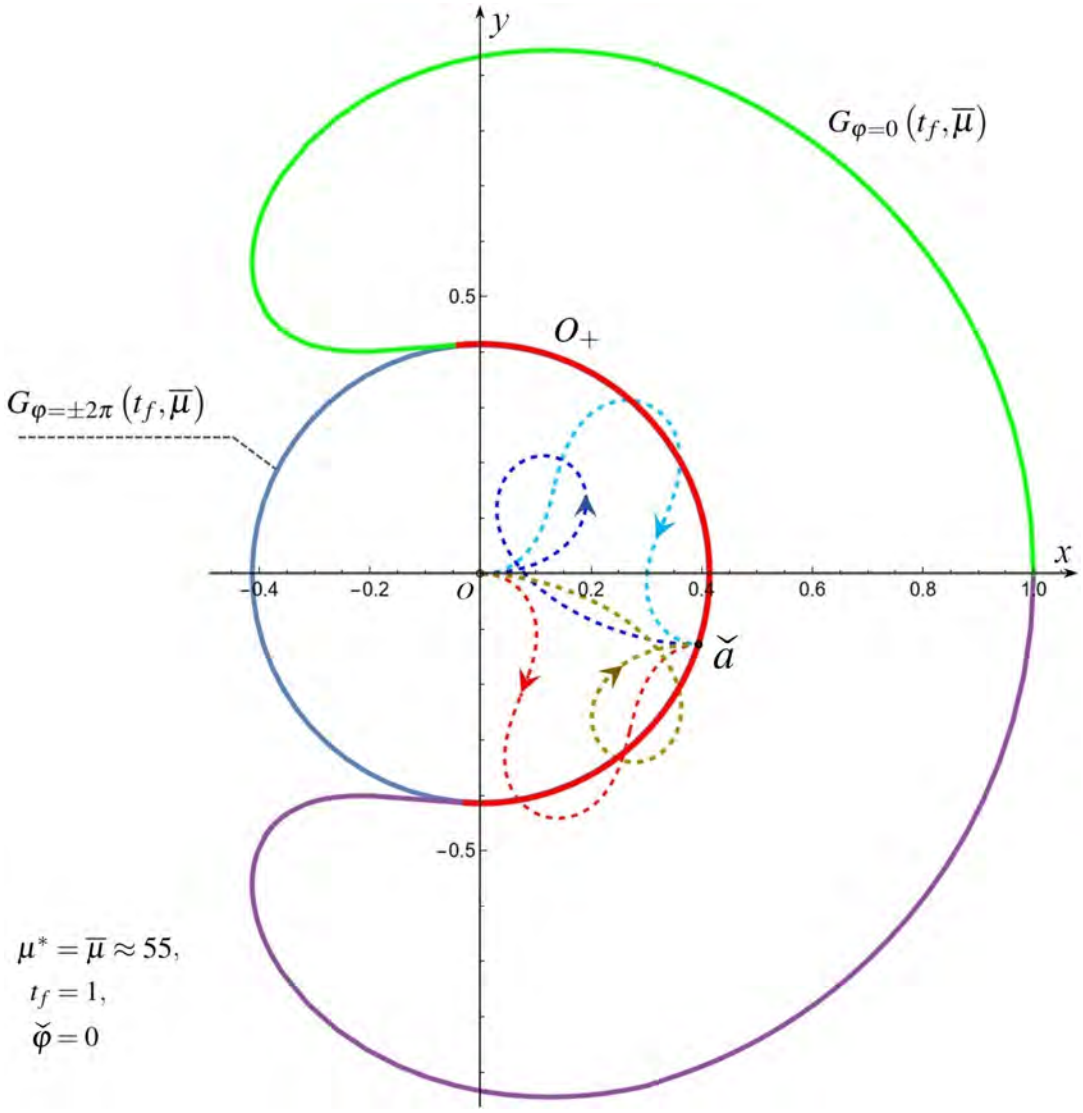

FIGURE 17. Four globally optimal Euler elasticae

The curve A_6 on the boundary of the φ-section $G_{\varphi=0}(t_f,\overline{\mu})$ is marked in red. The radius of the circular φ-sections $G_{\varphi=-2\pi}(t_f,\overline{\mu}) = G_{\varphi=2\pi}(t_f,\overline{\mu})$ is equal to approximately 0.41. Since the curves A_5 and A_6 coincide for $\varphi = 0$, two globally optimal elasticae lead to each point on them. One of these elasticae (for some point $\breve{a}$) is shown in red. It is generated by the control of the type U_6 with two instants of sign change. The other elastica is shown in light blue, and it is generated by the control type U_5 with two instants of sign changes also. The elastica, ending on the curve A_1 in the φ-section at $\varphi = 2\pi$, leads to the same point $\breve{a}$. It is generated by the control of the type U_1 and is depicted in dark blue. The fourth elastica leading to the same point is generated by the control of the type U_4 and is shown in yellow. Therefore, four globally optimal elasticae lead to the point under consideration. This property is valid for any point on the right semi-circumference O_+.

Thus, a consideration of φ-sections and a correct understanding of how their boundary is structured help to find and classify globally optimal elasticae and their quantity.

CONCLUSION

Based on the Pontryagin maximum principle and the specific properties of the kinematics of the Dubins car, the paper describes 6 types of open-loop controls that lead to the boundary of the three-dimensional reachable set $G(t_f,\mu)$ at a given time t_f under a given constraint μ on the integral quadratic expense of control. In essence, these 6 types are similar to those that were established earlier for the case of the geometric constraint on instantaneous control values. This made it possible to numerically construct the boundary of the reachable set.

We emphasize that the paper is in the nature of a numerical study of the three-dimensional reachable set under the integral constraint. Probably, many facts discovered numerically can be substantiated analytically. In particular, the fundamental question is an analytical description of the curves A_1, A_3, A_2, and A_6, the arcs of which form the boundary of the φ-sections of the reachable set for $\varphi \geq 0$.

Acknowledgements

The authors are thankful to the Reviewer for the very helpful remarks. L.V. Kamneva and A. Belan provided quite useful assistance in preparing the paper in English. The authors are grateful to them.

REFERENCES

[1] A. A. Ardentov, Y. L. Sachkov, Solution to Euler's elastic problem, Automation and Remote Control, 70 (2009) 633-643.

[2] A. A. Ardentov, Multiple solutions in Euler's elastic problem, Automation and Remote Control, 79 (2018) 1191-1206.

[3] L. Euler, Methodus inveniendi lineas curvas maximi minimive proprietate gaudentes, sive solutio problematis isoperimitrici latissimo sensu accepti, Geneva, Lausanne, 1744.

[4] M. I. Gusev, I. V. Zykov, On extremal properties of the boundary points of reachable sets for control systems with integral constraints, Proceedings of the Steklov Institute of Mathematics, 300 (2018) 114-125.

[5] K. G. Guseinov, A. S. Nazlipinar, On the continuity properties of the attainable sets of nonlinear control systems with integral constraint on controls, Abstr. Appl. Anal. 2008 (2008) 1-14.

[6] N. Huseyin, A. Huseyin, Compactness of the set of trajectories of the controllable system described by an affineintegral equation, Appl. Math. Comput. 219 (2013) 8416-8424.

[7] R. Levien, The elastica: a mathematical history, Electrical Engineering and Computer Sciences University of California at Berkeley, Technical Report No. UCB/EECS-2008-103, 2008.
[8] V. S. Patsko, S. G. Pyatko, A. A. Fedotov, Three-dimensional reachability set for a nonlinear control system, Journal of Computer and Systems Sciences International 42 (2003) 320-328.
[9] V. S. Patsko, A. A. Fedotov, Three-dimensional reachable set for the Dubins car: Foundation of analytical description, Communications in Optimization Theory 2022 (2022) 23.
[10] V. S. Patsko, A. A. Fedotov, Three-dimensional reachability set for a Dubins car: Reduction of the general case of rotation constraints to the canonical case, Journal of Computer and Systems Sciences International, 62 (2023) 445-468.
[11] Y. L. Sachkov, Closed Euler elasticae, Proceedings of the Steklov Institute of Mathematics, 278 (2012) 218-232.
[12] Y. S. Sikorskii, Elements of the Theory of Elliptic Functions: with Applications to Mechanics, KomKniga, Moscow, 2006. (in Russian).
[13] M. I. Zelikin, Theory and applications of the problem of Euler elastica, Russian Mathematical Surveys, 67 (2012) 281-296.